THESIS

BATTERY END-OF-LIFE CONSIDERATIONS FOR PLUG-IN HYBRID ELECTRIC VEHICLES

Submitted by

Eric Wood

Department of Mechanical Engineering

In partial fulfillment of the requirements

For the Degree of Master of Science

Colorado State University

Fort Collins, Colorado

Fall 2011

Master's Committee:

Advisor: Thomas H. Bradley

Anthony J. Marchese
Peter M. Young

ABSTRACT

BATTERY END-OF-LIFE CONSIDERATIONS FOR PLUG-IN HYBRID ELECTRIC VEHICLES

Plug-in hybrid electric vehicles (PHEVs) represent an advanced vehicle technology with the potential to displace petroleum consumption with energy generated on the US electric grid. While many benefits have been associated with the increased electrification of the US vehicle fleet, concerns over battery lifetime and replacement costs remain an obstacle to widespread PHEV adoption. In order to accurately determine the lifecycle cost of PHEVs, assessment studies must make use of informed assumptions regarding battery degradation and replacement. These assumptions should approach end-of-life (EOL) metrics not only in terms of pack level degradation but also loss of vehicle efficiency and performance in order to accurately represent consumer incentive for battery replacement. Battery degradation calculations should also remain sensitive to the range of ambient conditions and usage scenarios likely to be encountered in the US market. Degradation resulting from a single duty cycle has the potential to misrepresent battery life distributions for the US fleet.

In this study, the sensitivity of PHEV lifecycle cost to the battery replacement assumption is explored to underscore the need for an improved understanding of PHEV battery EOL conditions. PHEV specific battery test results are presented to evaluate the ability of industry standard life test procedures to predict battery degradation in PHEVs. These test results are used as inputs to a vehicle simulation program to understand changes in efficiency and performance with respect to battery degradation using a light commercial vehicle simulated as a blended-mode

capable, parallel PHEV20. A predictive battery degradation model based on empirical data is used to explore sensitivity of battery wear to various parameters including design variables, ambient conditions, and usage scenarios. A distribution of expected wear rates for a light-duty, midsize passenger vehicle modeled as a series PHEV35 is presented to highlight the uncertainty associated with battery life subject to US ambient conditions and driving distributions.

The results of this study show that active management of PHEV battery degradation by the vehicle control system can improve PHEV performance and fuel consumption relative to a more passive baseline. Simulation of the PHEV20 throughout its battery lifetime shows that battery replacement will be neither economically incentivized nor necessary to maintain performance. The spectrum of climate and usage conditions PHEVs are expected to face in the US market suggest that the assumption of a single average ambient condition for battery wear calculations may not be representative of observed behavior in the fleet. These results have important implications for techno-economic evaluations of PHEVs which have treated battery replacement and its costs with inconsistency.

ACKNOWLEDGEMENTS

My excitement for electric drive technology can be credited to the infectious nature of my advisor, Dr. Thomas Bradley. His guidance and support have been the driving force behind my graduate studies.

Battery life test data used in this report has been made available through a collaborative effort with the Electric Power Research Institute and Southern California Edison. In particular, I would like to thank Markus Alexander (EPRI) for assistance in data processing.

Detailed vehicle modeling software utilized in this report was developed by Benjamin Geller of Colorado State University. His knowledge of advanced vehicle modeling has been a source of great insight for my graduate research.

Predictive battery life modeling performed in this paper was made possible by Kandler Smith and Jeremy Neubauer of the National Renewable Energy Laboratory. Their insight into the nature of battery degradation has been invaluable.

Financial support for my graduate studies has been provided by the US Department of Transportation through the Dwight David Eisenhower Transportation Fellowship Program.

And a special thank you to my wife, Kayla, for her continued support of my professional aspirations. I could not have come this far without her.

Thank you,

Eric

TABLE OF CONTENTS

TABLE OF FIGURES

LIST OF KEY TERMS

ANL –	Argonne National Laboratory
BEV –	Battery electric vehicle
BOL –	Beginning-of-life
CARB –	California Air Resources Board
CD –	Charge depleting
CS –	Charge sustaining
DCS –	Degradation control strategy
DoD –	Depth-of-discharge
EOL –	End-of-life
EPRI –	Electric Power Research Institute
EV –	Electric vehicle
EVTC –	Electric Vehicle Technical Center
FAST –	Future Automotive Systems Tool
HEV –	Hybrid electric vehicle
HPPC –	Hybrid pulse power characterization
ICE –	Internal combustion engine
LA92 –	California Air Resources Board Unified Driving Schedule
MIT –	Massachusetts Institute of Technology
NAS –	National Academy of Sciences
NCA –	Graphite/nickel-cobalt-aluminum
NHTS –	National Household Travel Survey
NREL –	National Renewable Energy Laboratory
OEM –	Original equipment manufacturer
PHEV –	Plug-in hybrid electric vehicle
PNGV –	Partnership for a New Generation of Vehicles
RPT –	Reference performance test
SCE –	Southern California Edison
SOC –	State-of-charge
t-DoD –	Thermodynamic depth-of-discharge
t-SOC –	Thermodynamic state-of-charge
TMS –	Thermal management system
TMY3 –	Typical Meteorological Year Database 3
UDDS –	Urban Dynamometer Driving Schedule
US06 –	Supplemental Federal Test Procedure Driving Schedule
V2G –	Vehicle-to-grid
VMT –	Vehicle miles traveled
SEI –	Solid electrolyte interphase
USABC –	United States Advanced Battery Consortium
USCAR –	United States Council for Automotive Research

1. Introduction

Plug-in hybrid electric vehicles (PHEVs) are an alternative transportation technology capable of sourcing energy from both the electric grid and conventional gasoline [1]. By storing energy on board the vehicle in the form of electricity, PHEVs offer the potential to significantly reduce petroleum consumption, reduce greenhouse gas and criteria emissions, and improve US energy security. Following a full charge, PHEVs operate primarily on electricity for a nominal charge depleting (CD) range before switching to charge sustaining (CS) mode and operating on gasoline. The ability of a PHEV to meet vehicle power requirements in an all-electric mode is closely tied to pack power while the distance a PHEV can travel in CD mode is largely dependent on the available capacity of the pack. Packs with high power and energy density are advantageous for PHEVs as they increase the electric capabilities of the power-train without significantly impacting vehicle mass. A brief review of select automotive battery chemistry candidates is presented in Table 1 (data adapted from [2]).

Table 1. Comparison of automotive battery chemistries.

	Temperature (C)	Efficiency (%)	Energy Density (Wh/kg)	Power Density (W/kg)	Voltage (V)	Self-discharge (%/month)	Cost Estimate ($/kWh)
Lead Acid	-30 to 60	85	20 – 40	300	2.1	4 – 8	150
NiMH	-20 to 50	80	40 – 60	500 – 1300	1.2	20	500
Li-ion	-20 to 55	93	100 – 200	800 – 3000	~3.6	1 – 5	800

Lithium based technology has emerged in recent years as the chemistry of choice for PHEV batteries. Lithium technology provides the favorable aspect of relatively high energy density required of storage devices in PHEVs to achieve significant CD range. Additionally, lithium tends to exhibit superior cycle life compared to competitive technologies. Despite favorable cycle life, lithium still suffers from reduced utility subject to both age and cycling. The

impacts of age and cycling are evident both in terms of reduced power capabilities and a loss of available energy.

While PHEVs can be negatively impacted by loss of battery power and energy, they have the potential to mitigate the vehicle level effects of battery degradation through increased utilization of the internal combustion engine (ICE). While loss of pack capacity will cause the CD range of the vehicle to decrease, this is generally a small fraction of the total vehicle range. Hundreds of miles can still be accomplished by operating in CS mode. Control strategies that allow for blended operation between the electric motor and the ICE in CD mode also allow PHEVs to prevent loss of battery power from impacting total vehicle power.

The disconnect between battery degradation and loss of PHEV efficiency and power raises many questions. For instance:

- How has PHEV battery end-of-life traditionally been defined?
- Is PHEV battery end-of-life expected to be an indicator of consumer behavior regarding battery replacement?
- How can PHEV battery end-of-life be accurately predicted?
- What are anticipated levels of PHEV battery degradation in the US market?
- Will battery replacement be a necessary part of PHEV lifecycle costs?

This analysis will address these issues using lithium battery test data under a matrix of conditions. Test data will be used to inform models that will interpret the vehicle level impacts of PHEV battery degradation and predict battery wear based on a range of expected usage scenarios. To begin this analysis, a review of PHEV lifecycle studies is conducted, followed by a discussion of PHEV battery life testing and simulation methods used to determine battery life.

1.1. Impact of Battery Replacement on PHEV Lifecycle Cost

While PHEVs promise benefits to many elements of society, the market share that PHEVs will achieve in the near-term is dependent on their cost-competitiveness with

conventional vehicles. The incremental cost of PHEVs relative to conventional internal combustion vehicles is primarily associated with the costs of electric drivetrain and battery energy storage system. Advancements in electric drive technologies and the maturation of battery manufacturing systems will drive down PHEV prices with government incentives used to narrow the price gap in the interim, but the role of battery lifetime on PHEV incremental cost is uncertain.

The recent studies which have sought to quantify the incremental cost of PHEVs relative to conventional vehicles have been inconsistent in their assumptions as to whether PHEVs will require battery replacement during their useful life, a decision that has large effect on the lifecycle cost of a PHEV. In [3], the Electric Power Research Institute (EPRI) discusses the need for battery replacement by examining the distance required by battery warranties, the batteries usable state-of-charge (SOC), and how the vehicle's battery management system (BMS) handles degradation over time. Because the vehicles' lifecycle costs are sensitive to battery replacement, two sets of lifecycle costs are presented with each using different assumptions regarding replacement. A study by the Massachusetts Institute of Technology (MIT) assumes that no battery replacements will be necessary during a PHEV's useful life [4]. An Argonne National Laboratory (ANL) study presents lifecycle costs based on two different battery sizes; one in which a single battery replacement is required, and one sized such that replacement is not necessary [5]. EPRI's 2004 report [6] assumes no battery replacements in lifecycle analysis and justifies this claim with testing data, usage statistics, and technology improvement assumptions. The National Academy of Sciences (NAS) presents incremental costs of PHEVs without including the cost of battery replacement in a lifecycle costs analysis [7]. However, NAS does include battery life expectations that range from 3-8 years in the near term to 9-15 years by 2030; implying the need for battery replacement in a large percentage of PHEVs for years to come. In these 5 studies, the decision to include battery replacement in a lifecycle cost analysis increases the incremental cost of a PHEV by between 33% and 84%, as shown in Table 2.

Table 2. Impact of the battery replacement assumption on the incremental cost of PHEVs for various PHEV cost studies.

Organization (year)	Vehicle configurations	% Increase in incremental cost for one battery replacement
EPRI (2001)	PHEV 20, 60	52-71%
ANL (2001)	PHEV 30	33-47%
EPRI (2004)	PHEV 20	57-64%
MIT (2007)	PHEV 10, 30, 60	44-75%
NAS (2010)	PHEV 10, 40	39-84%

The battery replacement assumption has been demonstrated to significantly impact the lifecycle cost of PHEVs. In light of this large effect, a more detailed study of PHEV battery end-of-life (EOL) is required. In order to inform this study, industry standard EOL testing metrics as established by the United States Advanced Battery Consortium (USABC) are reviewed.

1.2. USABC Test Procedure and Thermodynamic State-of-Charge

The industry standard method for determining the lifetime and capabilities of automotive batteries is through USABC testing, but the applicability of USABC test procedures to the conditions of use of modern PHEVs is uncertain.

The USABC was formed in January of 1991 in an effort to promote the long term research and development of electrochemical energy storage systems. Currently operating under the guidance of the United States Council for Automotive Research (USCAR), USABC promotes collaboration between leaders of industry and academia in order to accelerate the development of high power and energy batteries for use in electric, hybrid, and fuel cell vehicles [8].

As part of its mission, the USABC publishes test procedures to guide the development of electrochemical energy storage systems. During its inception in the early 1990's, battery electric vehicles (BEVs) were receiving considerable attention from US automakers in anticipation of their commercial release. As such, USABC established battery testing procedures designed primarily for all-electric BEVs. These USABC standards established battery EOL for BEVs as

the stage at which specific failure criteria is met (e.g., capacity and/or power degradation). Specifically, when either:

> (1) "the net delivered capacity of a cell, module, or battery is less than 80% of its rated capacity when measured on the DST (Reference Performance Test); or
>
> (2) the peak power capability (determined using the Peak Power Test) is less than 80% of the rated power at 80% DoD,"

with DoD (depth of discharge) defined as:

> "the ratio of the net Ampere-hours discharged from a battery at a given rate to the rated capacity."

USABC last updated its battery EOL testing procedures in January of 1996 [9]. Since that time, vehicles have become far more sophisticated in their measurement and management of battery SOC; to the point that the USABC definition of EOL must be reexamined.

Conventionally SOC and DoD (where, DoD=1-SOC) are nameplate capacity-based, using a method known as Coulomb Counting to determine the percent of remaining charge relative to nameplate capacity [10]. Capacity-based SOC measurement is widely used in testing environments due to its high degree of stability and consistency; however, this method can be misleading as it does not represent the actual thermodynamic "state" of the battery [11] including Peukert effects, temperature effects, self-discharge, and capacity degradation. Modern BMS are now capable of taking these variables into account to determining a battery's thermodynamic SOC (t-SOC), where the t-SOC is a characterization of the battery with respect to its instantaneous chemical composition and extent of reaction [12]. The discrepancy between SOC and t-SOC in batteries of various ages can be seen in Figure 1.

Advancements in BMS systems have important ramifications for how modern PHEVs manage their batteries as the batteries degrade over the vehicle's lifetime. Electric vehicles built in the 1990's were designed to maintain their original range over their lifetime and as a result experienced accelerated power degradation once capacity degradation necessitated the use of the

battery under low t-SOC. Because PHEVs do not have so strict a requirement on battery capacity (as they are able to drive under a hybrid mode), PHEV degradation control strategies (DCS) are now capable of preventing a battery from being depleted to the point where this accelerated degradation occurs. This allows PHEVs to operate within a t-SOC "window" that supplies adequate battery power while avoiding the accelerated degradation which occurs at extreme t-SOC. The lower limit that a DCS places on t-SOC is especially critical to PHEVs as they will operate at low t-SOC for travel in CS mode.

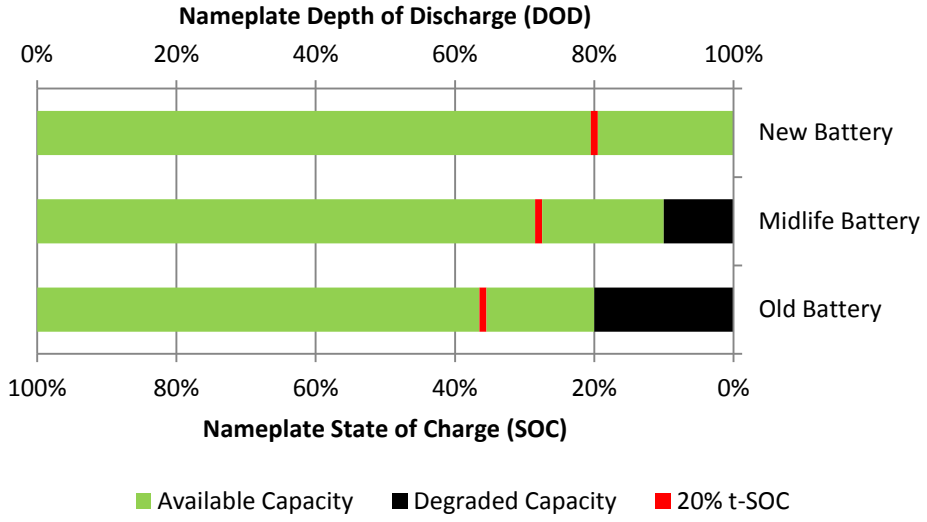

Figure 1. Variation of t-SOC as a result of capacity degradation.

1.3. Modeling PHEV Battery EOL

PHEV battery life has traditionally been predicted through the use of testing and simulation. While PHEV specific battery life test procedures have the ability to produce a high level of resolution with respect to the system level effects of battery degradation, there are significant drawbacks associated with using battery life testing to predict battery degradation in the fleet. Most notably, testing procedures are only capable of capturing the effects of individual duty cycles on a battery. Multiple testing schedules would be necessary to sweep the multi-dimensional space of ambient conditions and usage scenarios to which PHEV batteries are likely

to be subjected. When considering the substantial investment of time and capital necessary to perform a single test schedule, the notion of developing PHEV battery life estimations purely via testing immediately becomes cost prohibitive.

Battery life predictions under a matrix of conditions become feasible only through the use of modeling and simulation. High fidelity battery life simulation scenarios that capture varying ambient temperature profiles, battery sizes, and driving patterns are of great value to battery manufacturers and vehicle OEMs as they inform in the design process by constructing systems capable of maintaining acceptable utility for a desired period of time. These model based designs provide the benefits of reduced development time and cost through the use of optimization algorithms used to determine optimal battery chemistry, size, and thermal management. The two approaches generally applied to creating predictive battery degradation models are 1) physics-based and 2) empirical.

Physics-based models utilize analytical relationships describing chemical reactions in the battery to predict degradation resulting from specific fade mechanisms. Loss of battery power and energy can be attributed to a number of factors including: irreversible chemical reactions, mechanically induced fatigue, and thermal stress. These factors are generally superimposed making it difficult to isolate individual contributions to overall loss of power and energy. A summary of degradation mechanisms occurring at the cell anode as summarized by [13] is presented below in Table 3.

While physics-based models can be extremely accurate in predicting chemically induced reactions, they tend to be computationally expensive requiring simultaneous solutions to multiple partial differential and algebraic equations. This can complicate system design processes that seek to use a battery wear model as part of a larger iterative design process. Additionally, certain degradation mechanisms cannot be analytically described and the contributing nature of competing mechanisms is often difficult to predict.

Table 3. Summary of lithium battery degradation mechanisms occurring at the anode.

Cause	Effect	Leads to
Electrolyte decomposition	Loss of lithium impedance rise	Capacity fade, power fade
Solvent co-intercalation, gas evolution and subsequent cracking formation in particles	Loss of active material, Loss of Li	Capacity fade
Decrease of accessible surface area due to continuous SEI growth	Impedance rise	Power fade
Changes in porosity due to volume changes, SEI formation and growth	Impedance rise, over-potentials	Power fade
Contact loss of active material particles due to volume changes during cycling	Loss of active material	Capacity fade
Decomposition of binder	Loss of Li, loss of mechanical stability	Capacity fade
Current collector corrosion	Over-potentials, impedance rise, inhomogeneous distribution of current and potential	Power fade
Metallic lithium plating and subsequent electrolyte decomposition by metallic Li	Loss of lithium (Loss of electrolyte)	Capacity fade, power fade

Empirical models use experimental cycling and shelf life data to inform best fit equations that describe loss of power and energy. Equations can be fit based on optimal mathematical formulas and/or physically based phenomena. Empirical models are able to capture the effects of multiple degradation mechanisms over a range of storage and cycling conditions. These models tend to computationally efficient and are well suited to integration into larger vehicle system design algorithms. Despite these advantages, empirical models are limited to the spectrum of testing conditions used to generate the model. Care must be taken when applying empirical models not to exceed stated bounds of operation.

The current analysis makes use of empirical models that are both PHEV specific and constructed using more general test data for lithium batteries. A description of testing procedures used in this analysis is now presented.

2. Testing Procedures

The current analysis makes use of two testing data sets: 1) a PHEV specific data set generated in a collaborative effort by the EPRI and Southern California Edison (SCE) capturing over 4000 cycles and 2) a collection of battery test data (both calendar and cycling) organized by the National Renewable Energy Laboratory (NREL) to inform a predictive battery degradation model. A description of testing procedures used to generate these data sets is now provided.

2.1. Southern California Edison Test Conditions

Between 2005 and 2009, a PHEV battery pack was degraded in the laboratory over 4323 charge-discharge cycles using a PHEV-specific test profile. The battery test profile was developed to simulate the duty cycle of a PHEV battery in CD mode, in CS hybrid mode, and in recharging mode. The battery test profile was derived from a dynamic vehicle-level simulation of a portion of the INRETS URB1 vehicle test cycle. The battery test cycle replicates the urban driving conditions likely to be the most demanding to the battery (low speed, high acceleration and charge-sustained HEV mode at low battery SOC). Details of the battery and vehicle characteristics can be found in [14] and [15].

This PHEV specific test profile is made up of a series of CD, CS and charging modes to simulate the types of battery usage which are common to PHEVs.

2.1.1. Charge Depleting Mode Testing

The CD mode begins with a fully charged battery. The 181.5 second EV test profile (see Figure 2) was repeatedly applied to the battery until the battery voltage drops below a pre-defined threshold for 10 consecutive seconds. This threshold was determined at the beginning of the life cycle test to ensure that the battery SOC at the end of the CD mode was approximately 25%.

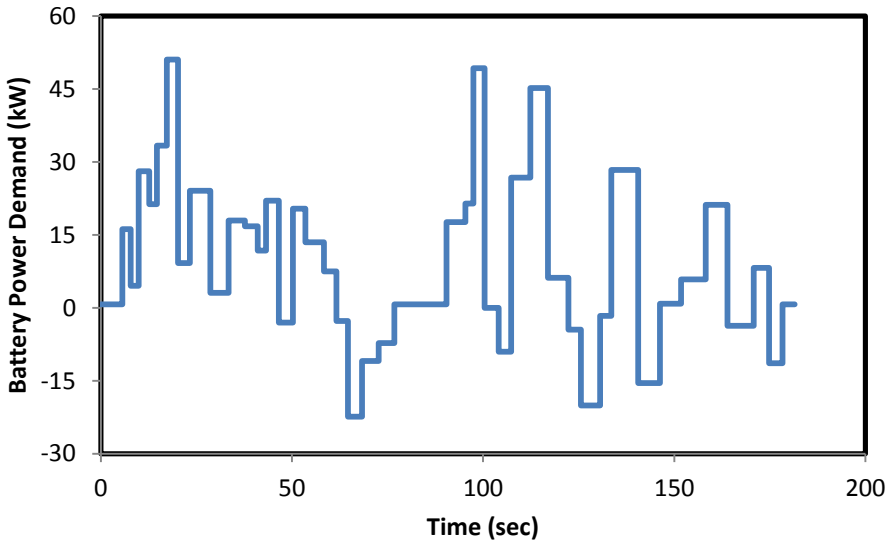

Figure 2. PHEV CD test profile used to define PHEV-specific battery degradation test procedure

2.1.2. Charge Sustaining Mode Testing

The CS mode starts at the completion of the CD mode. The 181.5 second HEV test profile (see Figure 3) was continually applied to the battery until the total duration of the CD mode and the CS mode reached a combined 2.6 hours (equivalent to a 50 mile trip). The battery was then allowed to rest for 15 minutes before the next mode.

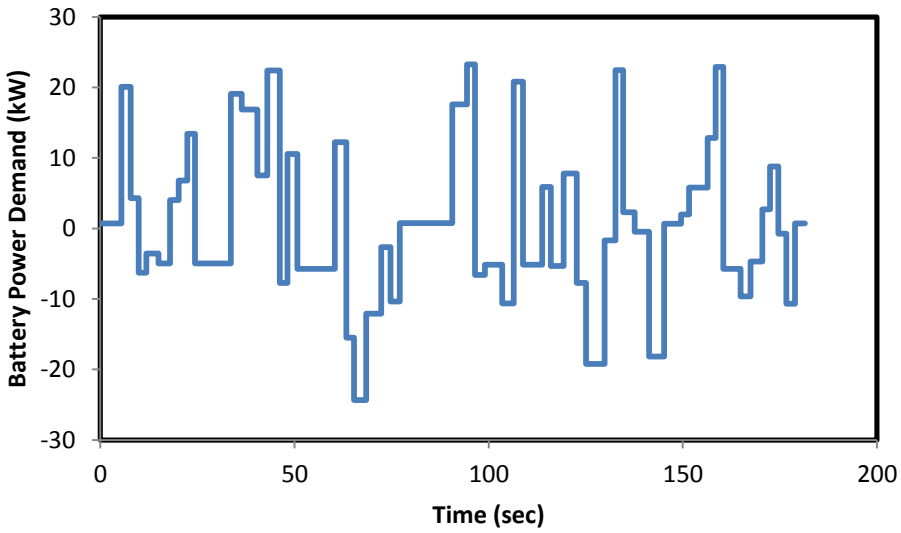

Figure 3. PHEV CS test profile used to define PHEV-specific battery degradation test procedure

In the CS mode, the battery SOC should remain constant. The test profile was adjusted to ensure a zero net energy transfer between the battery and the test equipment. A minor offset was applied to the test profile at the beginning of the life cycle test to guarantee a constant SOC during the CS mode. Throughout the course of the test, the SOC drifted as the battery's internal resistance changed due to degradation effects. When the balance of capacity in ampere-hours exceeded a pre-defined parameter at the end of any test profile, the SOC was readjusted automatically.

2.1.3. Battery Charging Mode Testing

After completion of the simulated driving profile, the battery was charged using the manufacturer's suggested charge algorithm (see Figure 4) at the highest rate that would not present any detrimental effect to the battery life (3.5 hrs for a full charge). At the completion of this mode, a rest period lasting approximately one hour was applied to allow for chemical and thermal stabilization before the start of a new test cycle.

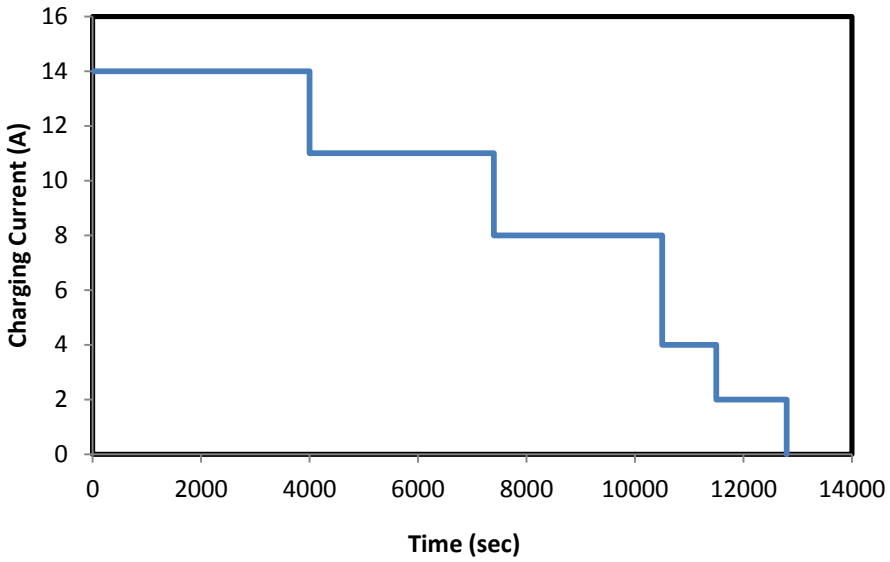

Figure 4. PHEV charging profile used to define PHEV-specific battery degradation test procedure.

2.1.4. Details of SCE Test Methods

This test profile was adapted by SCE to the test equipment at their Electric Vehicle Technical Center (EVTC) (see Table 4). The 6.3 hour cycle was applied to 3 PHEV modules (see Table 5 for specifications) continuously from March 2005 to August 2009 for a total of 4323 cycles.

Table 4. SCE EVTC battery degradation test equipment.

Make	Model	Description
AeroVironment Inc., Simi Valley, CA	ABC-150	Battery Cycler
Neslab, Oak Park, IL	HX-300	Recirculation Chiller
National Instruments, Austin, TX	PCi-CAN2 Series 2	CAN Communication Interface Card
AeroVironment Inc., Simi Valley, CA	SmartGuard Type E	12-bit data acquisition system

Table 5. PHEV battery module specifications.

Manufacturer	Saft
Battery Chemistry	Lithium Ion
Number of Cells/Pack	102
Number of Modules/Pack	17
Nominal Pack Voltage (VDC)	367
Cell Capacity (Ahrs)	41 @ C/3
Pack Energy (kWh)	15.5 @ C/3
Peak Pack Power (kW)	100
Module Dimensions (mm)	190 x 123 x 242
Pack Weight (kg)	136
Total System Weight (kg)	180
Charger	3.3 kW Conductive 208-240 VAC Input
Cooling	Circulated liquid at 25°C, Continuous 0.5 l min^{-1} flow
Battery Monitoring	SAFT BMS with voltage, current, and temperature sensing

Reference Performance Tests (RPTs) were conducted before the start of the life cycle test, and at periodic intervals every 240 test cycles (equivalent to approximately 2 months of testing) to characterize the performance of the battery. The following tests are included in each RPT:

- A constant current discharge at a rate of C/1
- A constant current discharge at a rate of C/3
- A peak power test
- A Hybrid Pulse Power Characterization (HPPC) Test (performed in the dual mode configuration)

The first three tests were performed using the methods of the USABC Electric Vehicle Test Procedure Manual [9]; the HPPC test was performed using the methods the Partnership for a New Generation of Vehicles (PNGV) Battery Test Manual [16]. A preliminary cycle, including a discharge at a constant current rate of C/3 down to 60% DoD and a full recharge, was performed prior to each RPT. A 30 minute rest was included in between each charge and discharge.

2.2. NREL Test Conditions

For the purpose of developing a predictive battery degradation model, NREL collected lithium life test data from multiple sources to describe resistance growth and capacity fade as a function of both storage and cycling [17]. Testing conditions for all datasets are described below in Table 6.

Table 6. NREL lithium life test dataset parameters.

	Storage Tests	Cycling Tests
Resistance Growth	T= 20, 40, 60 C SOC= 50, 100%	DoD= 20, 40, 60, 80% Charge voltage= 3.9, 4.0, 4.1 V Cycles per day= 1, 4
Capacity Fade	T= 0, 10, 23, 40, 55 C Voltage= 3.6, 4.1 V	DoD= 20, 40, 60, 80% Charge voltage= 3.9, 4.0, 4.1 V Cycles per day= 1, 4

The assembled dataset consists exclusively of cell level test data for lithium ion graphite/nickel-cobalt-aluminum chemistry. This particular chemistry is potentially well suited to automotive applications as it exhibits acceptable power density, energy density, and life characteristics. As such, the assembled data set is assumed to be representative of near term lithium technology for use in PHEV battery packs. Application of the assembled dataset to a predictive battery degradation model is outlined in section 0.

3. Modeling and Simulation Design

Using the two data sets generated from testing procedures described in Section 2, models were developed to 1) analyze effects of PHEV battery degradation on vehicle efficiency and performance and 2) understand the sensitivity of battery degradation to various usage, ambient condition, and vehicle design scenarios. The SCE test data was used as an input for battery parameters in a detailed vehicle simulation program to understand the vehicle level effects of battery degradation on a PHEV. The datasets organized by NREL were used to develop an empirical model of battery degradation in lithium packs. The predictive battery degradation model is supported by a high level vehicle simulation tool and a lumped parameter thermal vehicle model that predicts cabin and battery temperature based on ambient conditions and driving distance. Detailed descriptions of these two approaches are outlined below.

3.1. Detailed Vehicle Level Simulations

To determine the effects of battery degradation on PHEV attributes, a light commercial vehicle was modeled and simulated as a blended-mode capable, parallel PHEV20. A Modelica-based vehicle simulation environment representing the LFM (light, fast, modifiable) vehicle model presented in [18] was used to relate battery degradation to changes in vehicle performance. These simulations assume that calendar life degradation in practice is insignificantly different from calendar life degradation in the laboratory, that module-level performance degradation dominates over pack level effects such as module imbalance, and that the rate of battery degradation is independent of control strategy.

Simulations were performed using two DCSs: a “Static DCS” and a “Dynamic DCS”. The Static DCS maintained the SOC window in the battery such that the energy available for

discharge remained constant over the battery's life (equivalent to maintaining a constant, minimum capacity-based SOC over the lifetime of the vehicle). The Dynamic DCS allowed for a constant percentage of thermodynamic capacity to be utilized in CD mode such that the energy available for discharge was a function of the actual energy available in the battery instead of rated capacity (equivalent to measuring and recalibrating the minimum t-SOC continuously over the lifetime of the vehicle). The Dynamic DCS ensured that the vehicle entered CS mode at 25% t-SOC.

The vehicle model employed in these simulations represents a real vehicle which was designed so that the battery was not oversized in terms of its power output, thereby minimizing incremental costs. As such, any loss of battery power from original specifications would be immediately visible at the vehicle level. Modern PHEVs are designed with some battery power margin to allow for battery degradation without affecting the electrical power capability of the drive-train. As such, these degradation simulations represent a worst-case scenario.

3.2. Predictive Battery Degradation Model

In order to explore the sensitivity and variability of battery wear in PHEVs to various parameters, a predictive battery wear model was implemented. The life model is informed by vehicle power train and battery pack thermal modeling capabilities. It was possible to capture the effects of drive cycle based loading and ambient conditions on battery wear rates in a predictive and robust method. An overview of this integrated approach is provided, followed by an explanation of various design and usage scenarios employed.

3.2.1. Life Model

Battery aging is caused by multiple phenomena related to both cycling and calendar age. Battery degradation is accelerated with the DoD of cycling, elevated temperature, and elevated voltage exposure, among other factors. At the battery terminals, the observable effects of degradation are an increase in resistance and a reduction in capacity. These two effects can be correlated with power and energy loss that cause battery EOL in an application. Mechanisms for resistance growth include loss of electrical conduction paths in the electrodes, fracture and isolation of electrode sites, growth of film layers at the electrode surface, and degradation of electrolyte. Mechanisms for capacity loss include fracture, isolation, and chemical degradation of electrode material, as well as loss of cyclable lithium from the system as a byproduct of side reactions.

Under storage or calendar-aging conditions, the dominant fade mechanism is typically growth of a resistive film layer at the electrode surface. As the layer grows, cyclable lithium is also consumed from the system, reducing capacity. In the present model, resistance growth and lithium capacity loss are assumed to be proportional to the square-root of time, $t^{1/2}$, typical of diffusion-limited film-growth processes [19]. Under cycling-intense conditions, degradation is mainly caused by structural degradation of the electrode matrix and active sites. Cycling-driven degradation is assumed to be proportional to the number of cycles, *N*. Cell resistance growth due to calendar- and cycling-driven mechanisms are assumed to be additive:

$$R = a_o + a_1 t^{1/2} + a_2 N \tag{1}$$

Cell capacity is assumed to be controlled by either loss of cyclable lithium or loss of electrode sites,

$$Q = \min(Q_{Li}, Q_{sites}) \tag{2}$$

where

$$Q_{Li} = b_o + b_1 t^{1/2} \tag{3}$$

$$Q_{sites} = c_o + c_1 N \tag{4}$$

Models (1), (3), and (4) are readily fit to a resistance or capacity trajectory measured over time for one specific storage or cycling condition. Using multiple storage and cycling datasets, functional dependence can be built for rate constants $a_1(T, V, DoD)$, $a_2(T, V, DoD)$, $b_1(T, V, DoD)$, $c_1(T, V, DoD)$. The present battery life model was fit to laboratory aging datasets [20]-[23] for the lithium-ion graphite/nickel-cobalt-aluminum (NCA) chemistry as described in [23]. The NCA chemistry has generally graceful aging characteristics, and is expected to achieve 8 or more years of life when sized appropriately for a vehicle application.

The life model employed in this analysis was matched to experimental data for a NCA lithium-ion cell with up to 25% battery capacity fade. Beyond this level of wear, fade rates may accelerate, as sometimes evidenced by experimental data by a sharp drop in remaining capacity with continued cycling. The present life model does not capture possible accelerating fade mechanisms that could occur beyond 25% capacity fade.

Additionally, the life model has been shown to have weak sensitivity to normal battery temperature variation over the course of a single day. As such, this analysis uses average monthly temperatures as inputs to the life model in order to capture the effect of seasonal variability in disparate climate regions of the US.

While high heat generation rates resulting from aggressive driving are correlated to increased battery temperature, the impact of fast charging as it relates to rate-induced wear is not considered in the present model.

3.2.2. FAST Vehicle Model

Vehicle modeling was performed using a high-level tool developed by NREL known as FAST (Future Automotive Systems Tool). Analysis focuses on a PHEV with 35-mi (56-km) of nominal CD range followed by CS operation via a gasoline fueled ICE (PHEV35). Table 7 summarizes the component parameters selected for the PHEV35 model, which are roughly similar to the configuration of the production Chevrolet Volt [24].

Table 7. PHEV 35 FAST vehicle model inputs.

C_d	0.28
Frontal Area (m^2)	2.13
Vehicle Mass (kg)	1850
Engine Power (kW)	63
Motor Power (kW)	111
Battery Capacity (kWh)	16
Battery Max Allowable DoD	65%
Battery Max State of Charge	85%
Battery Thermal Management System	Liquid heating/cooling
Accessory Load (W)	300

Battery internal heat generation rates were correlated with drive cycles using cell-level test data for a representative Li chemistry. Nominal heat generation rates were determined using the California Air Resources Board (CARB) LA92 drive cycle, which was found to produce moderate heat generation rates characteristic of real-world drive cycles (see Table 8).

Table 8. Cycle attributes for tested cycles using PHEV35

	Cycle time, s	Cycle distance, km	Avg Speed, $km*hr^{-1}$	Avg Heat Generation Rate, W
UDDS	1369	11.99	31.5	103
LA92	1435	15.80	39.6	232
US06	600	12.89	77.8	622

3.2.3. Vehicle Thermal Model

In order to correlate ambient conditions to battery temperature, a detailed thermal vehicle model was implemented. Based on previous analysis done by NREL on a Toyota Prius [25], the thermal model captures both heating due to ambient temperature profiles and solar loading (see Figure 5). These inputs are merged with battery internal heat generation profiles during driving and charging to calculate average battery temperature over the course of a 24 hour period. In addition to passive-heat-transfer-to-ambient, the PHEV35 battery pack is equipped with an active thermal management system (TMS) capable of maintaining battery temperature within a desired band when driven or plugged-in.

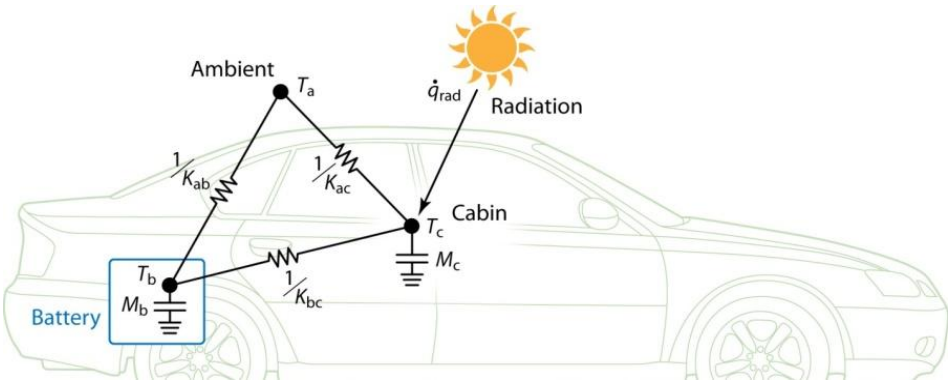

Figure 5. Vehicle thermal model employed to calculate battery temperature with respect to ambient temperature, solar loading, and thermal insulation.

Contributions to battery temperature in the PHEV35 are attributed to three sources: 1) ambient temperature, 2) solar loading and 3) heat generation plus active heating/cooling while driving. A baseline battery temperature is calculated as a difference above ambient due to solar loading (shown in Figure 6 in green). Heat generated during driving/charging and the effects of the active TMS are shown in red. The TMS is assumed to only operate when the vehicle is being driven or while plugged-in. All scenarios assume that the PHEV35 is left unplugged approximately 8 hours during the course of the day.

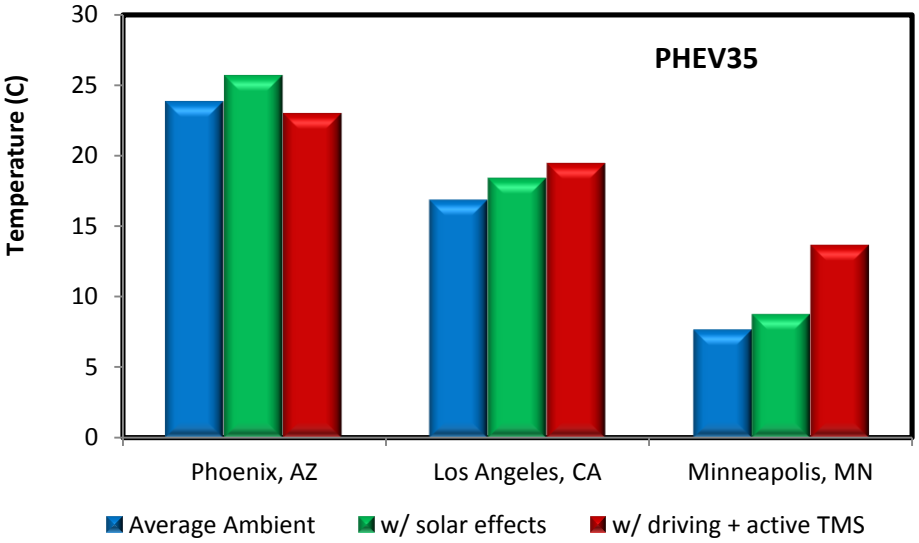

Figure 6. Battery temperature contributions from ambient, solar loading, active cooling, and internal heat generation.

While battery temperature calculations are performed to account for variations in driver aggression, active versus passive TMS, and daily distance, the cell level effects of temperature on internal resistance and capacity are not captured in the present model. For example, a battery pack in Minneapolis may experience significantly lower temperatures and subsequently reduced vehicle efficiency and CD range. Additionally, auxiliary loading placed on the PHEV35 resulting from operation of the active TMS with the potential to limit CD range are not considered. Auxiliary climate control loading has the potential to significantly impact the CD range of PHEVs as shown in [26]. Future analysis may address temperature effects on cell internal resistance and capacity to quantify the impact on PHEV efficiency and utility.

3.2.4. Initial Sensitivity Analysis

Upon successful integration of the battery life model, vehicle model and thermal model the PHEV35 was run through an initial sensitivity analysis to determine the conditions under which battery wear rates exhibited the greatest variability. A matrix of location, vehicle design, and usage scenarios was implemented with the primary outputs being battery resistance growth

and capacity fade at 8 years. Figure 7 and Figure 8 show the resulting variability of capacity loss and resistance growth for the PHEV35 (specific criteria can be found in Table 9).

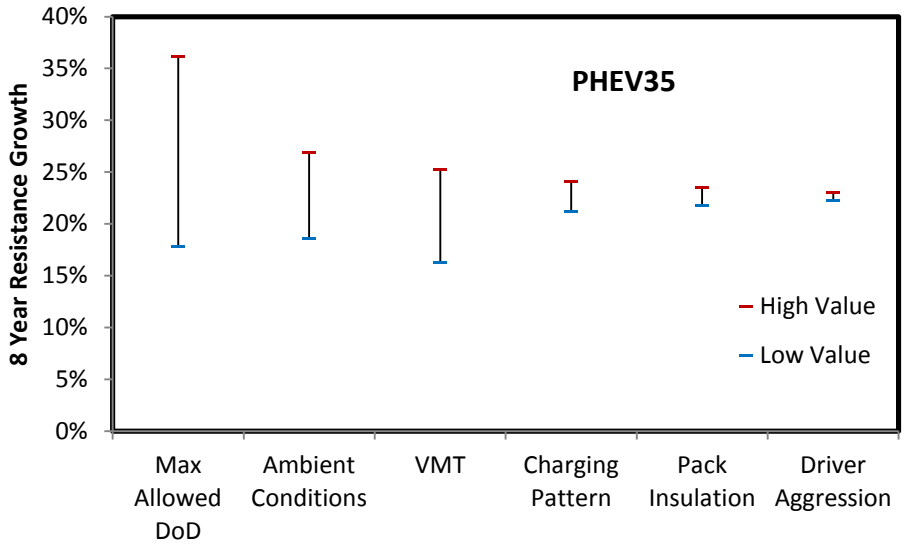

Figure 7. Battery wear sensitivity analysis for 8 year resistance growth on PHEV35.

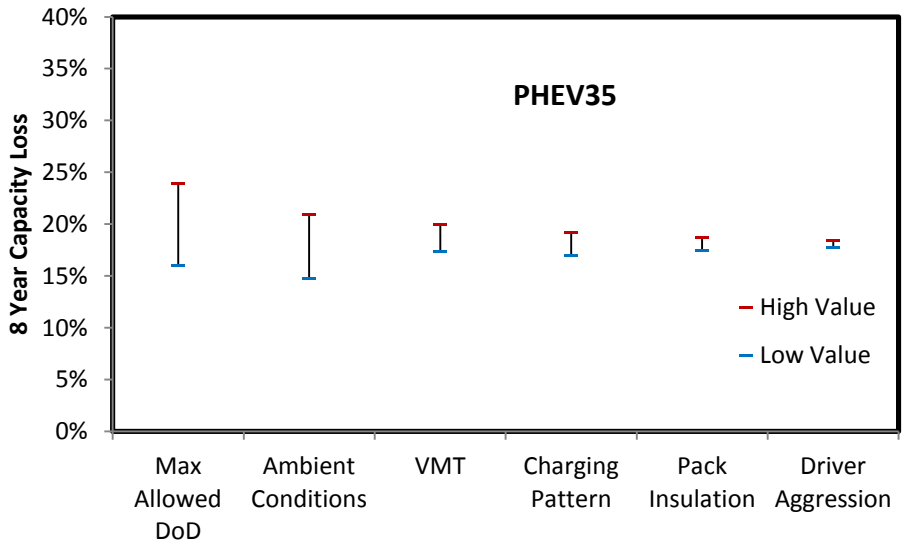

Figure 8. Battery wear sensitivity analysis for 8 year capacity fade on PHEV35.

Table 9. Design of experiments matrix for PHEV35 sensitivity analysis.

	Criteria producing greatest wear	Criteria producing least wear
Max Allowed DoD	87%	55%
Ambient Conditions	Phoenix, AZ	Portland, ME
Vehicle Miles Traveled	20,000 miles	5,000 miles
Charging Pattern	End-of-day	Just-in-time
Pack Insulation	Cabin dominated	Ambient dominated
Driver Aggression	US06	UDDS

Initial analysis indicates that ambient conditions and vehicle design parameters contribute significantly to variability of battery wear while usage patterns have a relatively minimal impact. The PHEV35 saw a limited impact on resistance growth relative to variation in charging pattern, pack insulation, and driver aggression (less than 3% for each). Note that the impact of fast charging is not considered in the present work.

After the initial sensitivity analysis, a more thorough investigation of the three conditions contributing the most uncertainty to battery wear was conducted. This analysis focuses on the effects of maximum allowable DoD, ambient conditions, and VMT. An explanation of the design of experiments is now presented.

3.2.5. Design of Experiments

After the initial sensitivity analysis, a more thorough investigation of the three conditions contributing the most uncertainty to battery wear was conducted. The PHEV35 analysis focused on ambient conditions, maximum allowable DoD, and VMT. An explanation of the design of experiments will now be presented.

3.2.5.1. Depth-of-Discharge

The effect of DoD on battery wear is explored for the PHEV35. The PHEV35 was assigned a nominal value for DoD and maximum SOC. These values are adjusted over a feasible range to explore the effect on wear (55-87% maximum allowed DoD). The SOC window of the

pack is adjusted relative to total energy to ensure that the available energy in the pack remains constant for all DoDs. By adjusting DoD and maximum SOC, the life model will capture the wear effects of deep cycling and operation at high voltages.

Adjusting pack energy has an impact on vehicle mass (and cost) and is subsequently related to CD range, efficiency, and acceleration. In light of these interactions, DoD was restricted to values that produced vehicle range, efficiency, and acceleration values within ±1% of the nominal design.

3.2.5.2. US Ambient Conditions

An expected distribution of wear rates was desired subject to US ambient conditions. Current HEV population data was used as an estimate for the future distribution of PHEVs. HEV population statistics highlight both large markets and regions where consumers have shown a tendency towards early adoption of advanced vehicle technology. The Polk Company's 2010 light duty vehicle registration dataset [27] was used to determine the top 100 US metropolitan areas in terms of number of HEVs (see Figure 9). These locations account for approximately 75% of the total US HEV population and represent a plausible estimate for the location distribution of PHEV early adopters.

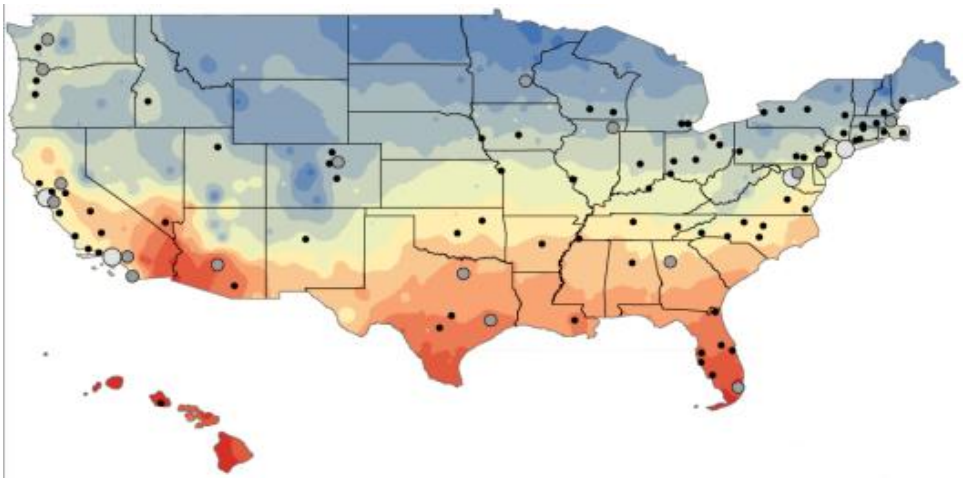

Figure 9. US metropolitan areas with large HEV populations overlaid onto average ambient temperature.

In addition to national temperature distributions, Los Angeles, CA was selected as a location for analysis based on its large share of the HEV market (see Table 10) and its moderate climate which produces battery wear representative of the US average.

Table 10. Top 5 US metropolitan areas in terms of HEV population.

Metropolitan Area	HEVs
Los Angeles, CA	149,042
New York City, NY	86,773
San Francisco, CA	82,756
Washington, D.C.	66,720
Chicago, IL	52,158

Ambient temperature and solar irradiation data was assembled from NREL's Typical Meteorological Year Database (TMY3) [28]. The national weighted distribution of average yearly ambient temperatures can be seen in Figure 10. TMY3 data was aggregated into monthly averages as hourly and daily battery temperature variations were shown to have a negligible effect on wear rates in the battery life model.

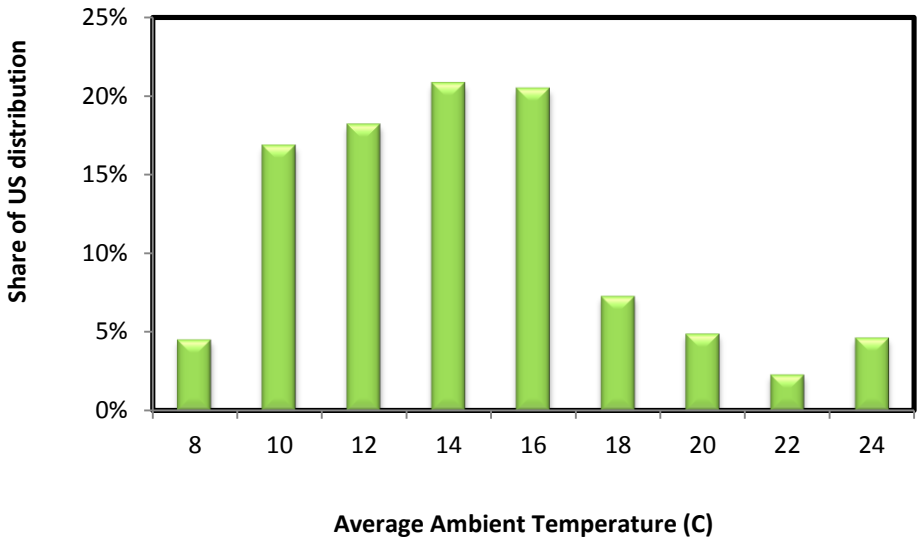

Figure 10. Distribution of average ambient temperatures for sampled US HEV population.

3.2.5.3. Vehicle Miles Traveled

Daily distance for each vehicle day was determined using the distribution of national averages according to the 2001 National Household Travel Survey (NHTS) [29]. Using this distribution, a zero mile per day probability was calculated as approximately 16% (about one day per week) such that the nominal VMT of the distribution was equal to 12,375 miles per year (19,916 km*yr-1).

Yearly VMT was adjusted from 5,000 to 20,000 miles per year (8,047 to 32,187 km*yr-1) to determine the effect of variable cycling on battery wear rates in the PHEV35. VMT was adjusted by scaling the NHTS distances while holding probability values constant as shown in Figure 11.

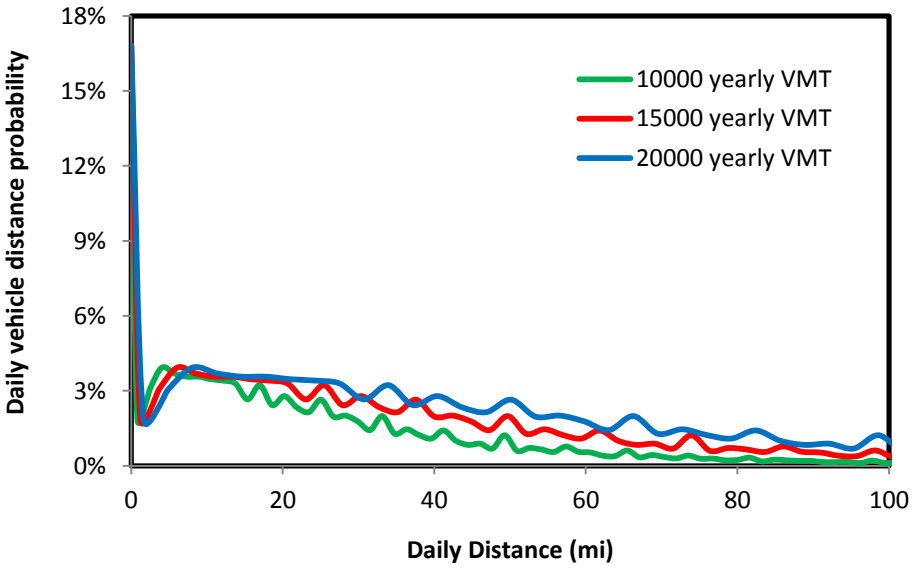

Figure 11. Daily distance distributions for three yearly VMT values.

This analysis uses fleet-aggregated driving distance statistics. Future analysis may quantify the effect of longitudinal vehicle distance driving distributions on battery wear. Longitudinal vehicle distance distributions track the driving behavior of individual vehicles over time and tend to exhibit a more focused set of distances with a small number of probability peaks representing routes frequently traveled.

4. Testing and Simulation Results

Results of multi-year life testing and simulations are presented in this section. PHEV specific battery test results are first presented to understand the effects of industry standard test procedure on PHEV battery EOL. Next, detailed vehicle simulation results are presented to correlate loss of battery power and energy with changes in vehicle level attributes for two DCSs. Lastly, predictive battery degradation simulation results are presented to illustrate the expected distribution of battery wear expected in the US market.

4.1. Southern California Edison test results

The results of the SCE RPTs are now presented as a function of cycle number to demonstrate the degradation of Lithium Ion batteries under PHEV specific test procedure. Battery EOL as calculated using the USABC capacity-based SOC can be contrasted with the battery EOL as calculated using t-SOC. In all of these results, no effort is expended to post-hoc separate cycling-based degradation from calendar life degradation.

4.1.1. Battery Degradation Test Results using Capacity-based SOC

This section presents testing results which illustrate how capacity degradation and power degradation develop under USABC tests which use a capacity-based SOC definition.

Figure 12 presents the battery RPT test results as measured during the battery degradation test. As shown in Figure 12, battery power degrades non-linearly with cycle number. This non-linear effect is especially evident after approximately 2400 cycles. Under the USABC testing procedure, the battery under test will reach EOL at approximately 3650 cycles due to power limit. The energy EOL is not reached in 4323 cycles under the USABC test at the C/3 discharge rate.

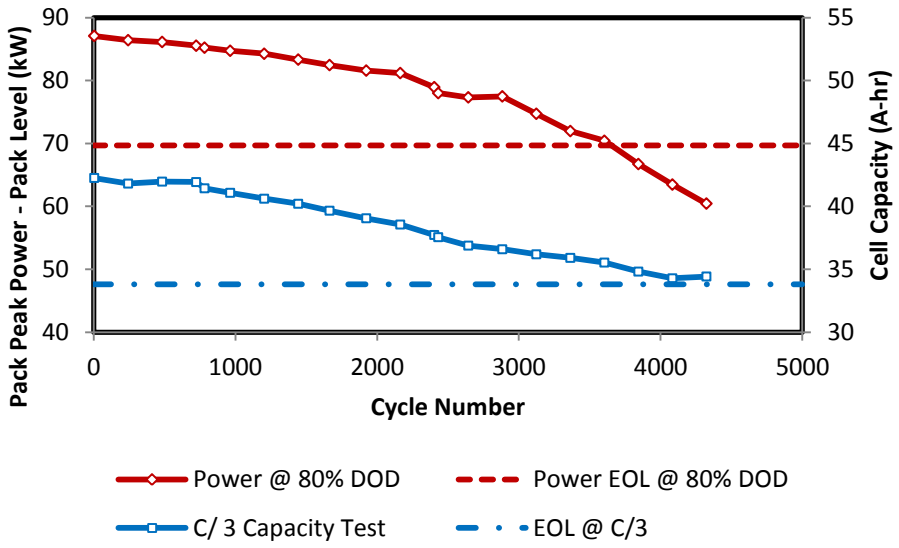

Figure 12. Energy and power measurements as a function of cycle number.

The effect that t-SOC has on power degradation rate can be seen in Figure 13 where degradation at various capacity based SOC are compared. Power can be seen to degrade at comparable rates for the three DoDs until approximately 2400 cycles. At that point, power measured at 80% DoD begins to rapidly degrade while power measured at 70% and 60% DoD continues to degrade linearly.

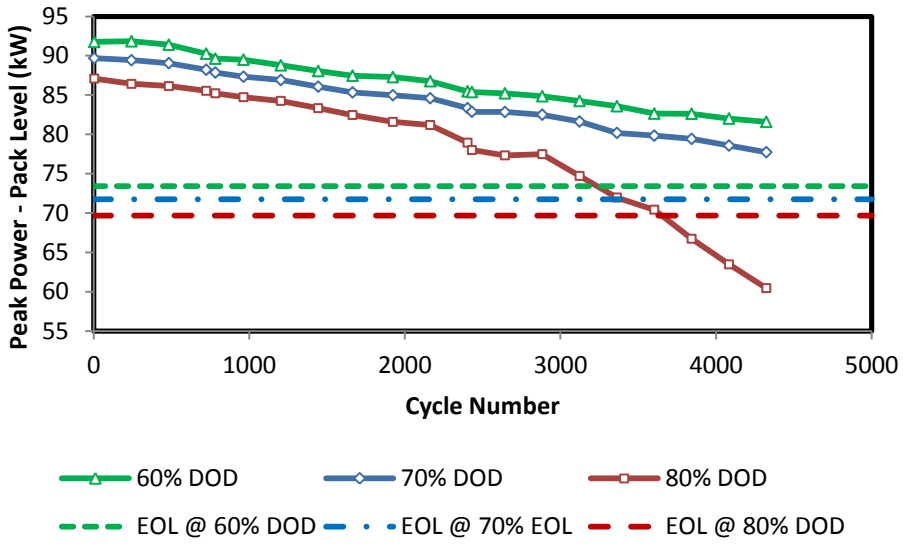

Figure 13. Power degradation at various levels of capacity based DoD as a function of cycle number.

A similar effect can be seen in Figure 14 which shows the battery internal resistance as a function of SOC and cycle number. Again, the pack internal resistance at low capacity-based SOC is increasing nonlinearly with cycle number after approximately 2400 cycles.

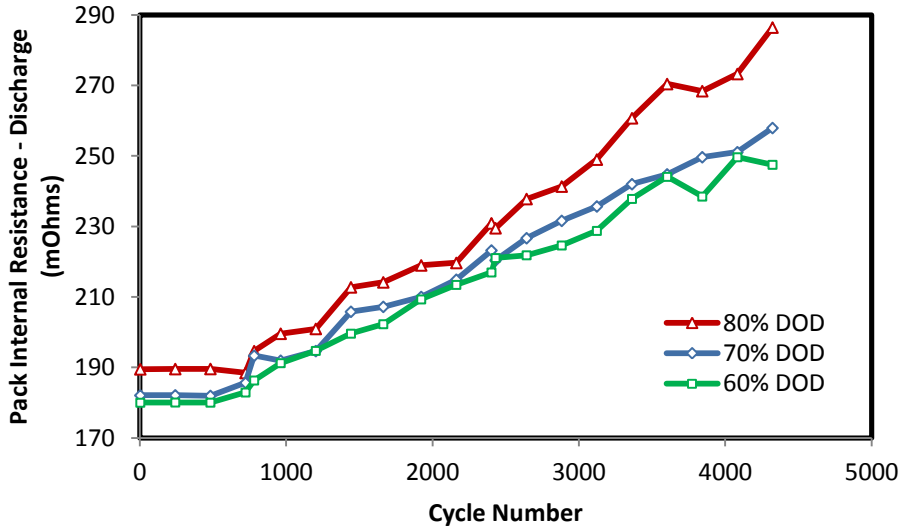

Figure 14. Pack internal discharge resistance as a function of cycle number.

This acceleration in degradation rate which is evident in all test results at low capacity-based SOC can be attributed to a significant change in the t-SOC that power is being measured at. As the battery capacity degrades, an 80% DoD corresponds to a lower and lower t-SOC condition, as seen in Figure 15. At approximately 2400 cycles, the degraded battery capacity forces the 80% DoD power test to occur at a t-SOC below 15%. This low t-SOC region has high impedance reaction pathways, increasing the internal resistance of the battery system and decreasing its peak power. In other words, the USABC test procedure mixes the effects of battery capacity degradation with those of battery power degradation; as the battery capacity degrades, the low SOC power tests begin to occur at lower and lower t-SOC.

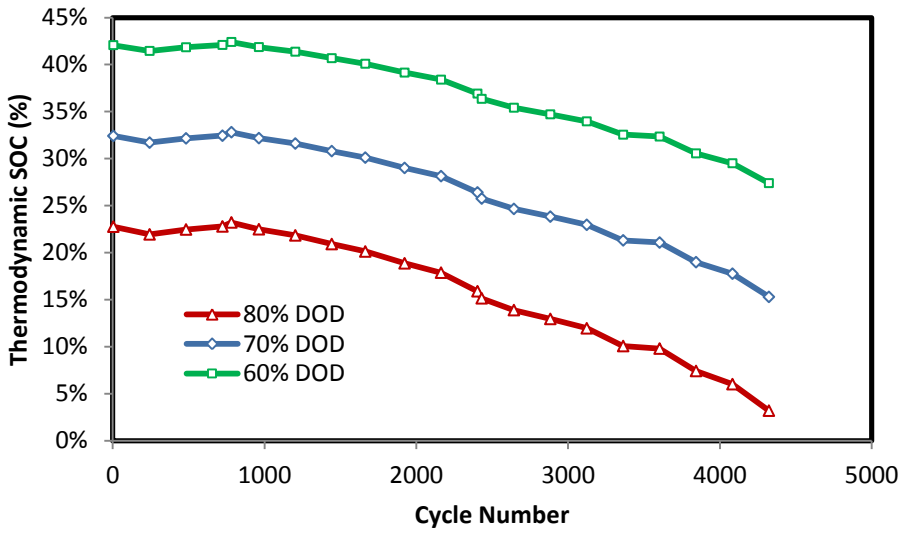

Figure 15. Thermodynamic SOC relative to capacity based DoD as a function of cycle number.

These types of results will be familiar to students of battery degradation under USABC procedures, but the results' relevance for evaluating battery EOL must be considered carefully. For BEVs, these USABC EOL definitions can be relevant because BEVs are expected to maintain a constant driving range (approximately proportional to battery nameplate capacity) throughout their lifetime. In addition, battery power at the vehicle's maximum range is important for the usability, drivability and consumer acceptability of the BEV. For PHEVs, the battery performance plays a more minor role in these functions of the vehicle. Because PHEVs can vary their energy management and control strategy by varying engine turn-on conditions and charging power demands, they can maintain the usability, drivability and consumer acceptability and can avoid battery EOL despite degrading battery capacity.

4.1.2. Battery Degradation Test Results using t-SOC

In this section, we analyze the same battery degradation test data so as to understand the ability of an advanced DCS to extend the life of PHEV batteries beyond USABC EOL. For this analysis, results of the previously presented RPTs were recalibrated to represent low power

testing at 20% t-SOC, as opposed to the USABC-required 20% SOC testing procedure. It should be noted that results presented in this section reflect testing that occurred for CD cycling from 100% to 25% SOC. This analysis does not account for differences in degradation rates as a result of CD cycling from 100% to 25% t-SOC. While cycling based on t-SOC is believed to extend battery life, an additional 5 years of testing would be necessary to fully account for the unique degradation mechanisms associated with test procedure based solely on t-SOC.

Figure 16 shows power and energy degradation measured at 20% t-SOC. This adjustment causes power to degrade more linearly as compared to the degradation presented in Figure 12. Instead of battery EOL being determined by power degradation, it is now dictated by energy degradation. This extends the battery life from approximately 3650 cycles to over 4400 cycles, an increase of over 20%.

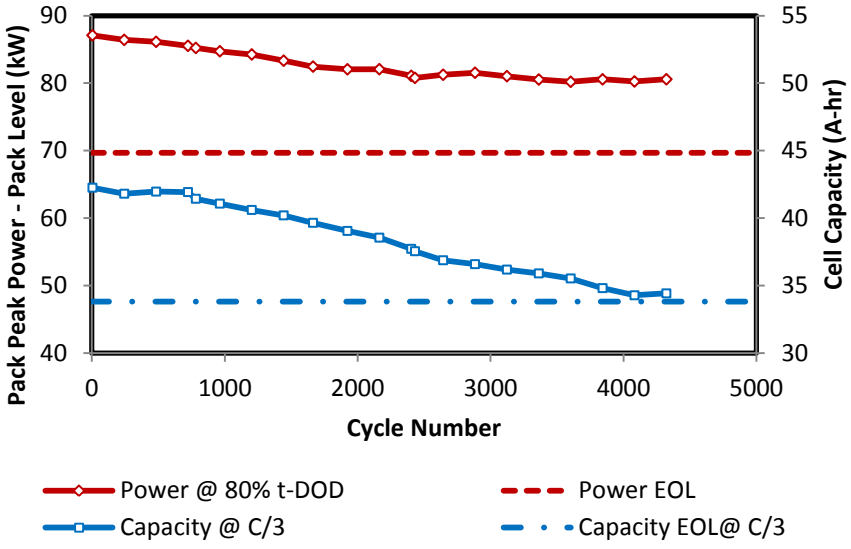

Figure 16. Energy and power measurements made at 80% DoD and 80% t-DoD as a function of cycle number.

Further evidence of the effect of measuring power degradation at uniform t-SOC can be seen in Figure 17. Power can now be seen to degrade at similar rates for all three t-DoD with degradation rate remaining relatively constant throughout testing.

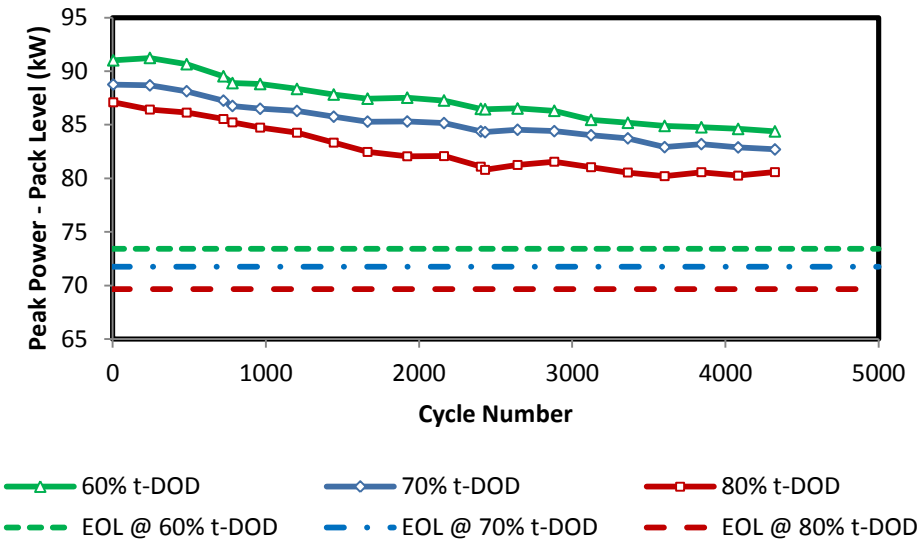

Figure 17. Power degradation measured at various t-DoD as a function of cycle number.

Figure 18 shows the effect that t-DoD measurements have on internal resistance as batteries degrade. Internal discharge resistance can now be seen to increase more uniformly and linearly for all conditions of t-DoD.

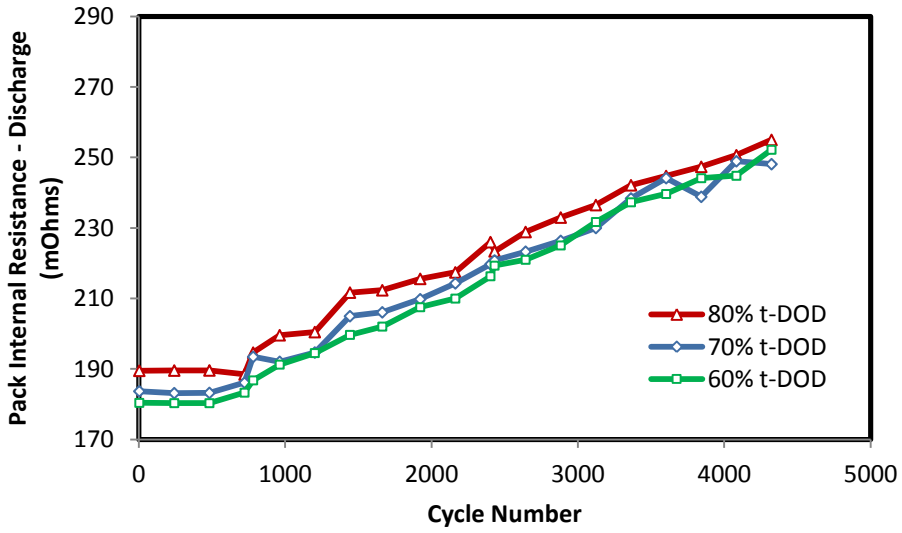

Figure 18. Pack internal discharge resistance as a function of cycle number.

These results indicate that the USABC test procedure underestimates the cycle life capability of battery systems which can compromise on the requirement to discharge to a

capacity-based SOC. Battery systems in PHEVs should be able to use an advanced DCS to avoid battery discharges at very low t-SOC, thereby increasing the battery cycle life.

4.2. Detailed Vehicle Level Simulation Results

Vehicle simulation results are presented for the PHEV20 in terms of fuel consumption, performance, and lifecycle cost.

4.2.1. Vehicle Fuel Consumption Simulations

Using the two DCSs, we can see in Figure 19 how fuel consumption is affected by battery degradation. PHEV fuel consumption is presented in this paper using an equivalent liter per 100 kilometer metric where electric power consumption in the vehicle is converted to gasoline consumption using the lower heating value for gasoline. CD and CS fuel consumptions are weighted based on vehicle's utility factor (UF) as defined in SAE J1711 [30]. PHEV UF is calculated as the ratio of the distance a PHEV travels in CD mode to the total distance traveled prior to a charging event. SAE J2841 [31] is used to predict UF based on CD range. Finally, composite fuel consumption is calculated by weighting urban and highway fuel economy based on EPA standards (55% urban and 45% highway measured using federal driving schedules) [32].

Figure 19 shows that the Dynamic DCS is able to reduce the increase in vehicle fuel consumption over the life of the battery pack. Over the 4323 cycles tested the Dynamic DCS fuel consumption increases by 25% compared to an increase of 32% using the Static DCS. This effect is due in part to the Dynamic DCS allowing the vehicle to operate in a higher SOC window where available battery power is superior. While the Dynamic DCS offers lower fuel consumption, it is also more susceptible to losses in CD range. Over the tested cycles, the Composite UF for the Dynamic DCS decreases by 13% while the Static DCS increases by 11%. While an increase in CD Range for degraded batteries may seem counterintuitive, it is a result of the Static DCS

maintaining the SOC window in CD mode. As the peak power of the battery decreases with use, additional distance is necessary to deplete a constant amount of battery capacity.

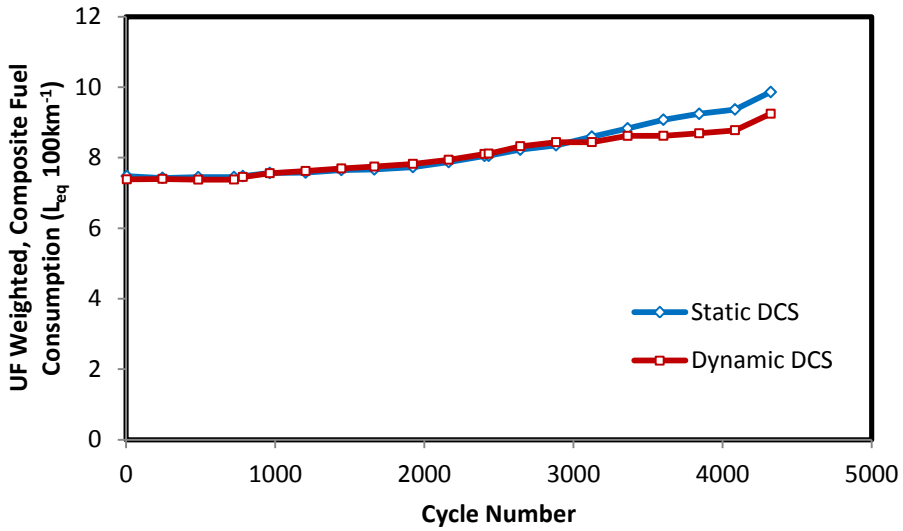

Figure 19. PHEV20 fuel consumption as a function of cycle number.

Additional understanding of battery degradation's effect on fuel consumption can be garnered by examining its effects on specific modes of operation and drive schedules. Figure 20 and Figure 21 display fuel consumption for the simulated PHEV20 broken into CD versus CS operation and urban versus highway drive schedules respectively. In both instances the scenario that relies more heavily on battery power is more efficient over the life of the battery. However, CD and urban fuel consumption increase more rapidly than CS and highway fuel consumption because of their reliance on battery power. In all cases the Dynamic DCS is able to maintain fuel consumption more effectively (see Table 11).

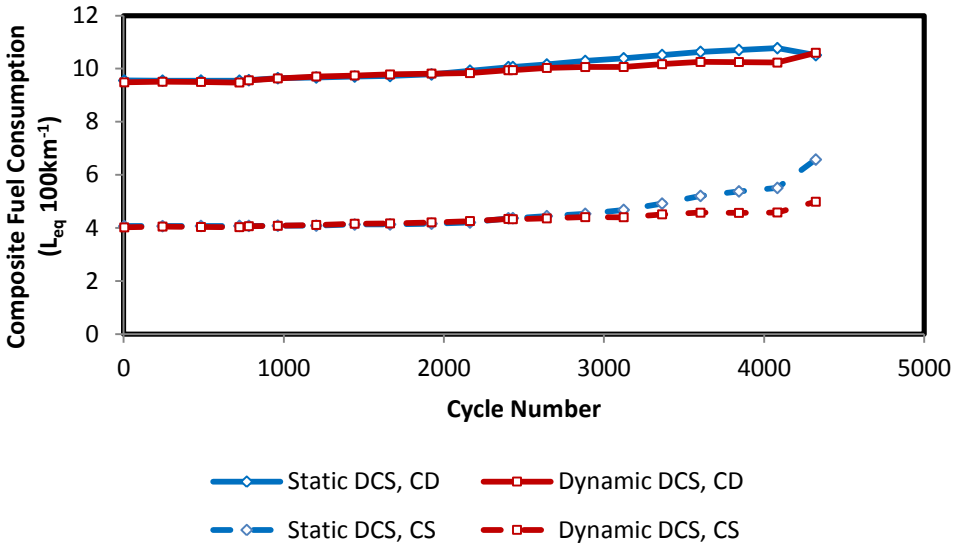

Figure 20. Composite fuel consumption as a function of cycle number.

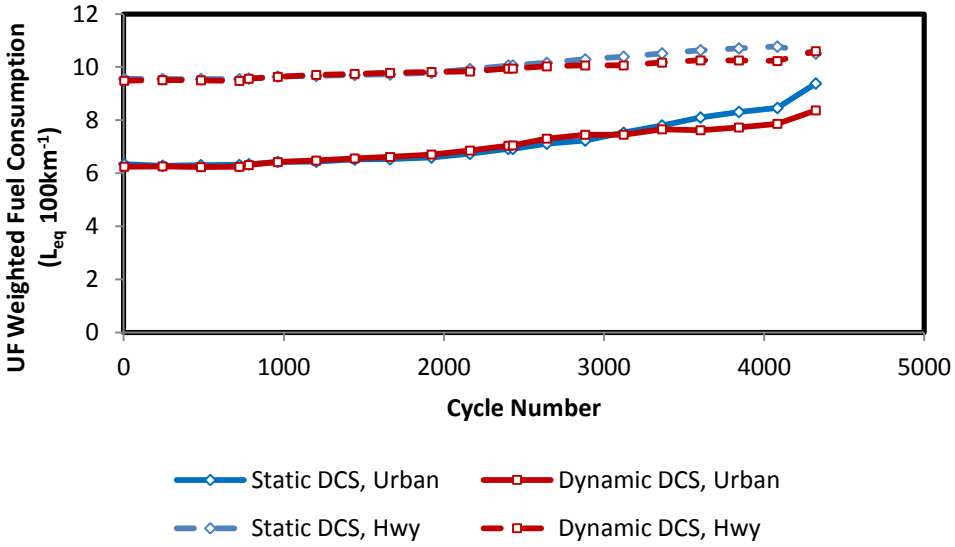

Figure 21. UF-weighted fuel consumption as a function of cycle number.

4.2.2. Vehicle Performance Simulations

Regarding performance, Figure 22 shows full-throttle standing acceleration times to 60 mph (96 kph) for the simulated PHEV20 as its battery degrades. It can be seen that in a blended parallel architecture, the simulated PHEV20 is able to maintain its acceleration time well for high SOC. However, acceleration does suffer slightly at low SOC. The acceleration time at 30% SOC

and 30% t-SOC increased by 57% and 36% respectively over the 4000+ cycles tested. While this increase is measurable, the vehicle would still be very drivable after 4000+ cycles, becoming relatively sluggish only at low SOC.

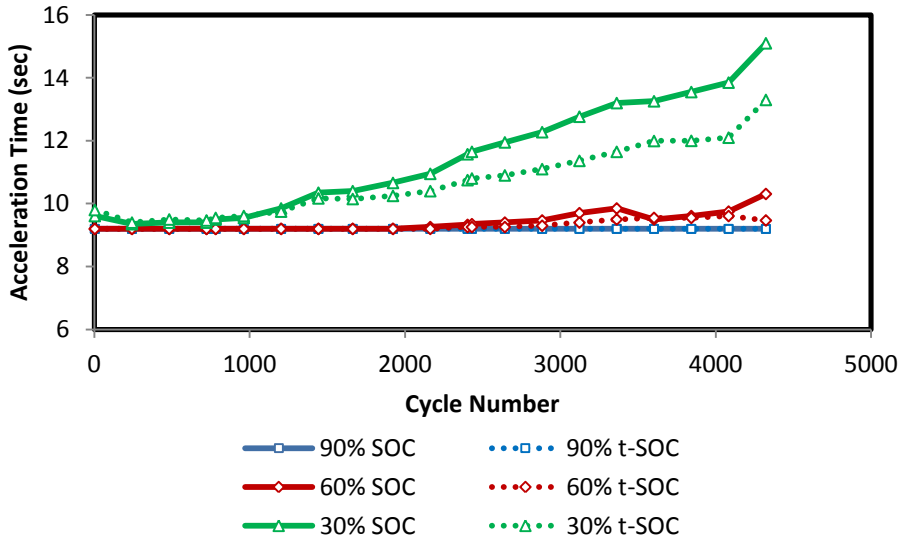

Figure 22. Full throttle standing acceleration to 60 mph (96 kph) time as a function of cycle number for multiple SOC.

The vehicle level effects of battery degradation have been presented in this section. We have shown PHEV fuel consumption to increase by 32% and 25% respectively for the Static DCS and the Dynamic DCS over the course of 4323 CD cycles. For comparison, testing conducted at Idaho National Laboratory has shown HEV fuel consumption to increase by 4.2%-14.7% over the course of 160,000 miles [33]. Acceleration times were simulated for 90%, 60%, and 30% SOC and t-SOC with increases in acceleration time presented in Table 11.

Table 11. Changes in equivalent fuel consumption, composite utility factor (UF) and acceleration time between cycle 1 and cycle 4323 for the simulated PHEV20 using Static and Dynamic DCS.

	Δ Static DCS	Δ Dynamic DCS
UF Weighted, Composite L_{eq} $100km^{-1}$	32%	25%
Composite CD L_{eq} $100km^{-1}$	62%	24%
Composite CS L_{eq} $100km^{-1}$	23%	14%
UF Weighted Urban Leq 100km-1	48%	34%
UF Weighted Highway L_{eq} $100km^{-1}$	10%	12%
Composite Utility Factor	11%	-13%
0-60 mph (96 kph) @ 90% SOC (t-SOC)	0%	0%
0-60 mph (96 kph) @ 60% SOC (t-SOC)	12%	3%
0-60 mph (96 kph) @ 30% SOC (t-SOC)	57%	36%

4.2.3. Vehicle Lifecycle Cost Simulations

Given the present state of battery technology, battery costs, energy prices, and personal driving patterns, it is highly unlikely that the majority of PHEV owners will be interested in battery replacement as a means of financial savings.

The fuel consumption results of the vehicle simulations were input into a vehicle total cost of ownership model. Inputs to the model include the changes in fuel consumption relative to battery degradation presented earlier in this paper, projections for future US energy prices [34], projections for lithium-ion battery prices [35], and a constant value of 15,000 for vehicle miles traveled (VMT) per year. VMT was modeled as being constant over time in order to represent the behavior of a high mileage driver maintaining the use of a PHEV over several years. This is meant to simulate the use of a PHEV most likely to benefit from a battery replacement. The presented model does not assign a salvage value to batteries that are replaced. While a future market for the second use of automotive batteries has been discussed [36], the current absence of such a market makes salvage value projections uncertain.

Figure 23 presents the results of a present value cost of ownership model reflecting the financial benefit of replacing a PHEV battery pack. The incremental costs of battery replacement after 10 years of ownership are not recuperated over a 25 year lifetime of the vehicle.

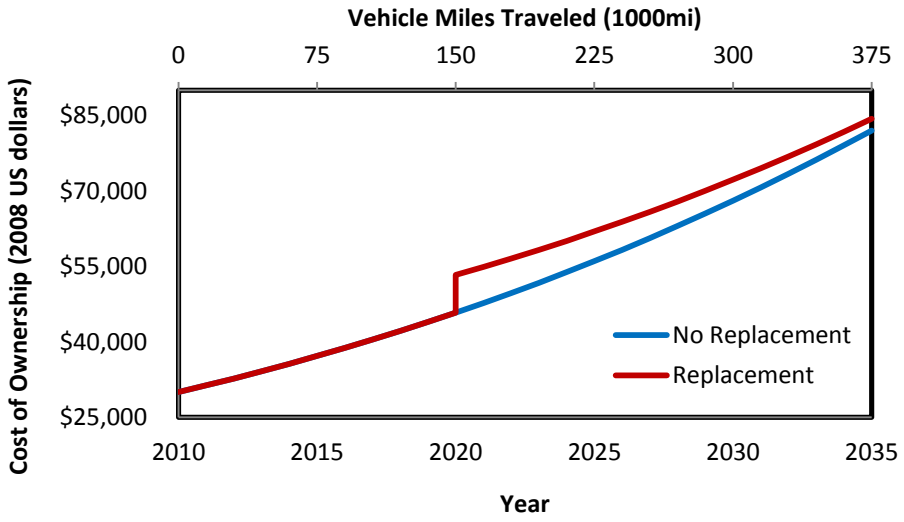

Figure 23. Cost of ownership model demonstrating the cost of battery replacement in PHEVs.

Using this model, battery replacement in a ten year old PHEV would have a payback period of greater than 15 years, potentially exceeding the life of the vehicle. While the payback period is sensitive to model parameters (degradation rate, replacement year, etc.), the conclusion that battery replacement is not economically incentivized is robust to a variety of scenario definitions. The potential financial benefit anticipated as a result of battery replacement is not expected to be sufficient incentive for a consumer or fleet manager to invest in a multi-thousand dollar battery pack replacement.

It is also unlikely that consumers will be interested in battery replacement for improved performance or increased drivability. While acceleration times have been shown to increase at low SOC, the simulated PHEV20 was still able to complete urban and highway drive cycles in CS mode at 4323 cycles with adequate performance, including the aggressive US06 drive cycle.

Replacement based on vehicle performance degradation would only be anticipated after the battery pack has endured far more than 4323 CD cycles.

4.3. NREL PHEV35 simulation results

The PHEV35 was simulated to determine battery wear for three conditions: 1) maximum allowable DoD (55-87%), 2) distribution of US ambient conditions, and 3) range of VMT (5,000-20,000 miles per year).

4.3.1. Depth-of-Discharge

Battery wear sensitivity to DoD was explored for the PHEV35. All battery sizes allowed the vehicle to discharge 10.4 kWh of energy from the battery and achieved consistent CD range, acceleration, and efficiency values to within ±1% of the baseline case. Figure 24 shows resistance growth and capacity loss at 8 years for a range of battery sizes.

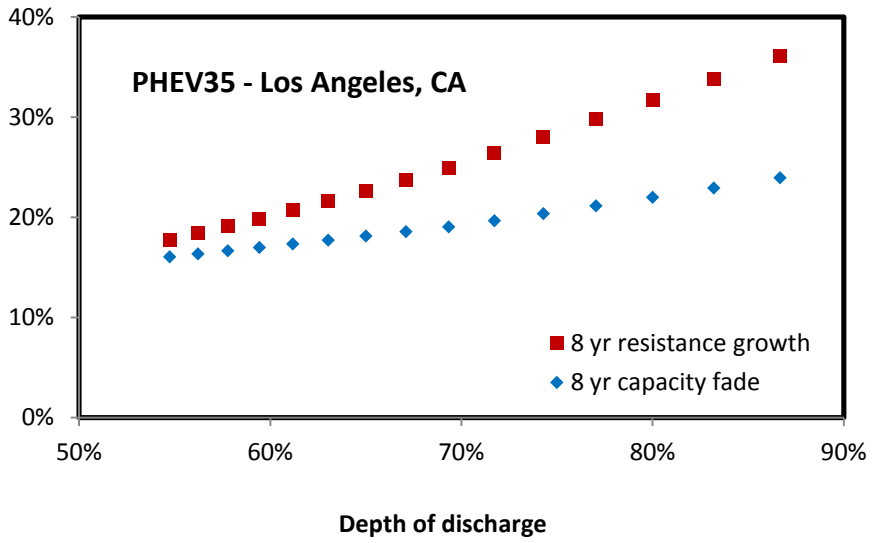

Figure 24. 8 year resistance growth and capacity loss for PHEV35 plotted against DoD.

Increasing the DoD window of the PHEV35 from 55 to 87% increased resistance growth by 18% while capacity loss increased by 8% over the same range. As the DoD window is expanded, increased resistance growth limits the power capability of the pack. Loss of pack

power would be reflected at the vehicle level in an increased degree of blended electric/petroleum operation or reduced all-electric vehicle power. This trend is reflected in the PHEV35 achieving reduced amounts of CD range at full power subject to increased DoD (see Figure 25). Full power is defined as the ability to discharge at the maximum beginning-of-life (BOL) power without violating the terminal voltage limit.

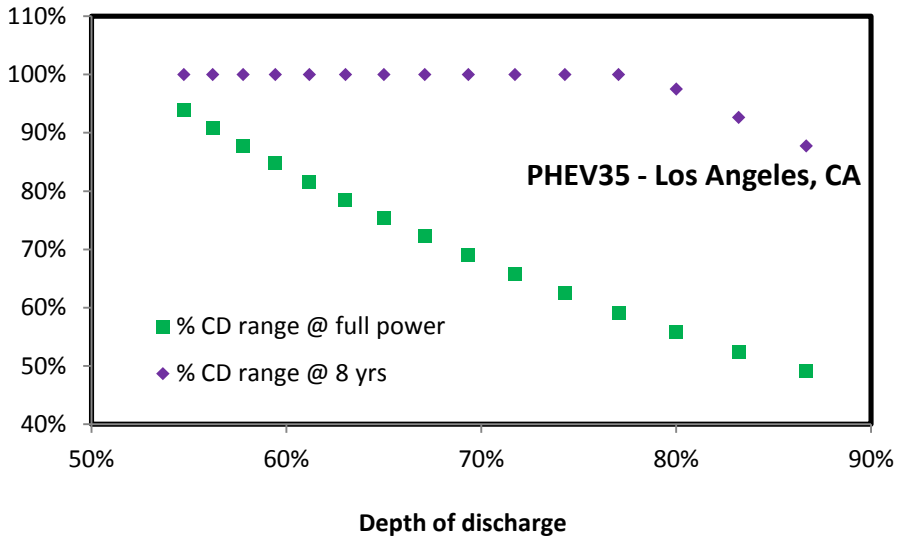

Figure 25. 8 year values for PHEV35 percent BOL CD range and percent BOL CD range at full power as a function of DoD.

Increasing DoD from 55 to 87% can be seen to decrease the percent of BOL CD miles that can be achieved after 8 years by 12% while the percent of CD miles that can be achieved at full power decreases by 45%. Using near term battery prices ($700/kWh production cost [37]) the difference in BOL battery price is approximately $5000 between the 55% and 87% DoD cases.

Standalone simulations needed to determine the DoD required to achieve 100% of BOL CD range at full power after 8 years were run for the PHEV35. It was determined that a PHEV35 pack with an approximate DoD of 50% could achieve BOL targets after 8 years of use for both CD range and CD range at full power. This design would represent an increase in pack cost of over $3000 relative to the baseline scenario of 65% DoD.

4.3.2. US Ambient Conditions

Resistance growth and capacity fade distributions after 8 years of use for the PHEV35 subject to US ambient temperatures and average driving distributions can be seen in Figure 26 and Figure 27. The PHEV35 can be seen to exhibit a relatively tight wear distribution. Resistance growth ranges from 18-26% and capacity loss ranges from 14-20% over 8 years, subject to variation in ambient temperature.

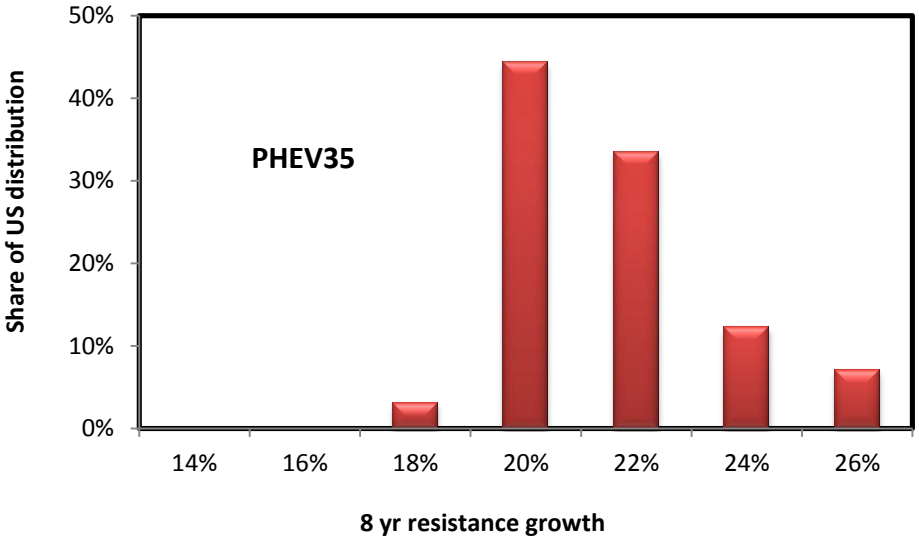

Figure 26. Distribution of 8 year resistance growth for PHEV35.

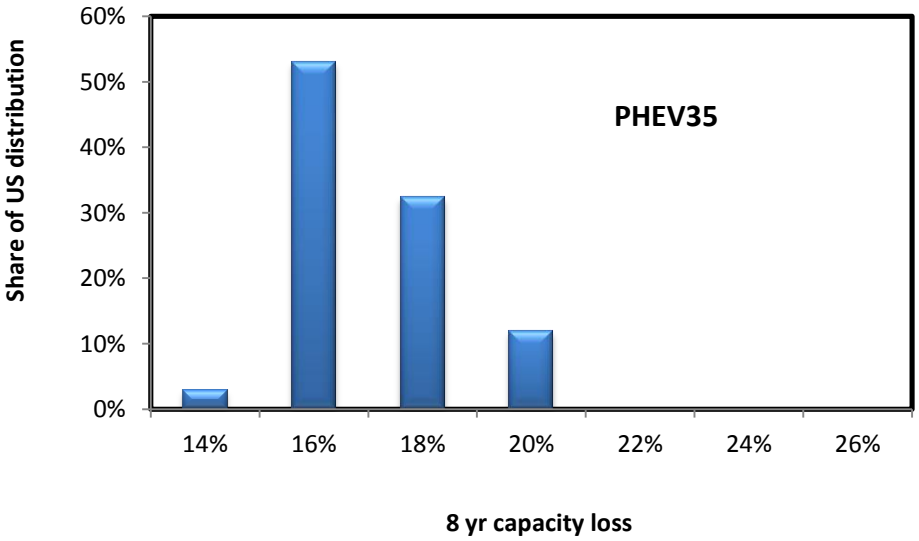

Figure 27. Distribution of 8 year capacity loss for PHEV35.

The general uniformity of the PHEV35 wear distribution can be attributed to the ability of the active TMS to regulate battery temperature in disparate climates. Figure 28 shows the distribution of battery temperatures experienced by the PHEV35 when exposed to US ambient conditions. By reducing average battery temperatures and minimizing the effect of ambient conditions on the battery, the active TMS in the PHEV35 allows for reduced wear rates with relatively low amounts of variability with respect to regional climate differences experienced in the US.

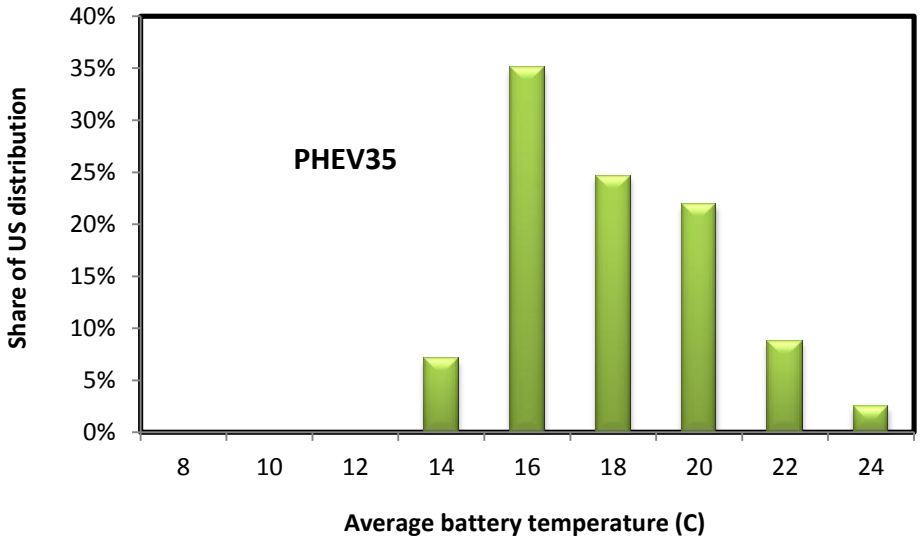

Figure 28. Distribution of average yearly battery temperatures for PHEV35 with US ambient and national driving distributions.

Additionally, the PHEV35 simulated in this analysis used a low enough DoD and experienced minimal capacity fade to allow for no loss of BOL CD range at 8 years of operation (for all US climates). This resulted in all PHEV35s achieving over 53,000 CD miles (85,600 CD km) of operation during their first 8 years.

4.3.3. Vehicle Miles Traveled

The PHEV35 was subjected to an array of annual VMT scenarios. Battery wear was calculated for annual VMTs from 5,000 to 20,000 miles (8,047 to 32,187 km*yr-1). Figure 29

shows the results of this analysis in terms of resistance growth and capacity fade after 8 years subject to ambient conditions in Los Angeles, CA.

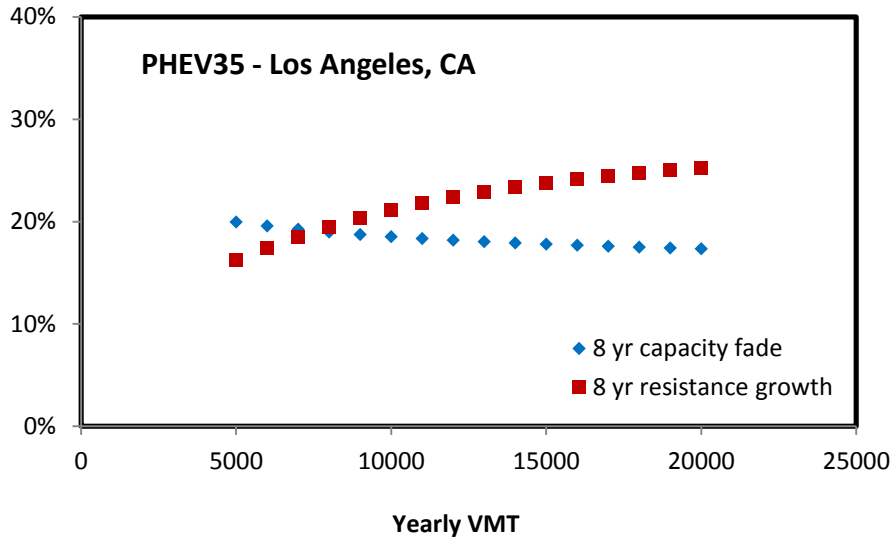

Figure 29. 8 year resistance growth and capacity loss as a function of annual VMT for PHEV35 subject to ambient conditions in Los Angeles, CA.

Increased VMT can be seen to have opposing effects on resistance growth and capacity loss in the PHEV35. Eight year resistance growth increases by 9% over the selected range of VMT while capacity fade actually decreases by 2% at high VMT.

In the life model, capacity loss is dictated by the greater of two fade mechanisms, calendar and cycling. In this case, calendar fade is the dominate mechanism driven by high voltage exposure. By increasing VMT, the battery is allowed to spend greater amounts of time at lower voltages which extends calendar life and thus reduces capacity fade. While the simulated phenomena of reduced capacity fade at high VMT has not been directly validated via testing, the competing effects of calendar and cycling fade on capacity loss lead the author to believe that the impact of PHEV VMT on capacity fade will be relatively muted.

While resistance growth increases at high VMT, the rate of growth can also be seen to decrease with high VMT. High VMT scenarios require more of the vehicle operation to shift from

CD mode to CS mode, where the latter mode causes relatively little incremental resistance growth in the battery.

VMT was found to have a minimal effect on CD range and the percent of CD range achievable at full power after 8 years. CD range at 8 years was 100% of its BOL value for all tested VMTs while the percent of BOL CD range that can be achieved at full power only decreases by 1% when increasing VMT from 5,000 to 20,000 miles per year.

5. Conclusions

Two PHEV platforms have been implemented in this study (the PHEV20 and PHEV35 respectively) to analyze the vehicle level effects of battery degradation and understand the sensitivity of battery wear to variations in ambient conditions, vehicle design, and consumer usage. Conclusions resulting from each analysis will now be summarized.

5.1. PHEV End-of-Life

A variety of studies assume that PHEV battery life can be predicted by the USABC cycle life test procedure; this assumption has dramatic effects on PHEV lifecycle cost and consumer acceptability. This study has shown how a DCS can be designed to extend battery life in PHEVs beyond USABC EOL. The effects of battery degradation on a blended parallel PHEV20 have been presented both in terms of vehicle efficiency and performance. In light of these effects, it is unlikely that the USABC definition for battery EOL will be predictive of how consumers and vehicle manufactures will approach battery replacement in PHEVs.

PHEVs differ from BEVs in that a direct relation between battery performance and vehicle performance does not exist. PHEVs can be designed to sense degradation and subsequently increase the degree to which they are blended to make up the power difference necessary to meet performance requirements. With this understanding, PHEV battery replacement would only make sense when a significant improvement in efficiency and/or performance could be achieved. In terms of fueling costs, replacement would be justified when the present value of fuel savings a battery replacement would provide is greater than the present value of replacement cost. This definition does not provide economic justification for pack replacement, even in scenarios involving significant battery degradation. In terms of battery replacement to restore as-

new acceleration performance, the justification for battery replacement based on improvement in vehicle performance is more subjective. While the improvement in acceleration a battery replacement provides can be quantified, the amount of improvement that justifies an expensive battery replacement is an individual decision.

Finally, as a result of the disconnect between existing testing procedures and modern PHEV battery requirements and control capabilities, USABC should consider revising testing procedures for the specific application of PHEVs. Future work should anticipate the desire of automotive manufactures to design intelligent DCS that allow for adequate performance over the vehicle's life while avoiding battery replacement.

5.2. Battery Degradation Sensitivity

Sensitivity of battery wear to ambient conditions, vehicle design, and usage patterns has been explored for the PHEV35. This analysis has shown that the spectrum of climate and usage conditions PHEVs are expected to face in the US market suggest that the assumption of a single average ambient condition for battery wear calculations may not be representative of observed behavior in the fleet.

Ambient conditions have been shown to have a large effect on battery wear for the PHEV35 simulated in this study. The effects of ambient conditions on battery life can be mitigated by appropriate vehicle design. Thermal insulation and TMSs can be designed to regulate temperature and extend battery life.

DoD was found to significantly impact battery wear. Resistance growth and capacity fade were significantly reduced by designing a pack to operate with a relatively low DoD. However, pack design for low DoD can increase vehicle up-front costs by requiring additional total energy to achieve a desired CD range. For the modeled PHEV35 the extra battery capacity required for a 55% vs. 87% DoD window represents a roughly $4900 increment in pack cost. Increased battery

energy may also require components such as the electric motor to be resized to maintain vehicle acceleration.

Consumer usage behavior was found to have a relatively low impact on battery wear. The modeled PHEV35 saw minimal impact on battery wear due to charging pattern (end-of-day versus just-in-time) or driving aggression. Increasing VMT on the PHEV35 from 5,000 to 20,000 miles per year (8,047 to 32,187 km*yr-1) was found to decrease the percentage of CD range achievable at full power by 1%.

Future work on battery wear prediction may focus on improving the 8 year achievable CD VMT estimations for the PHEV35 vehicle platform. Incorporating effects of temperature on pack internal resistance and capacity is expected to reduce the achievable CD VMT for PHEVs in cold climates as vehicle range is compromised at low pack temperatures. Alternatively, utilizing longitudinal driving statistics (such as those developed using NREL's Transportation Secure Data Center) could allow analysis to focus on driving patterns well suited to potential PHEV users. Daily distance distributions with low deviation and averages below the CD range of the PHEV could improve 8 year achievable VMT estimations. Additional analysis may also seek to develop a range of potential near term V2G scenarios to determine the subsequent impact on battery wear.

6. References

1. T.H. Bradley, A.A. Frank, Renew. Sustain. Energ. Rev. 13 (2009) 115–128.

2. F.V. Conte, Electrotechnik & Informationstechnik, (2006) 123/10: 424-431.

3. Electric Power Research Institute, Comparing the Benefits and Impacts of Hybrid Electric Vehicle Options, Palo Alto, California, 2001, 1000349.

4. Laboratory for Energy and the Environment, Electric Powertrains: Opportunities and Challenges in the U.S. Light-Duty Vehicle Fleet, Sloan Automotive Laboratory, Cambridge, Massachusetts, 2007, LFEE 2007-03 RP.

5. Argonne National Laboratory, Hybrid Electric Vehicle Technology Assessment: Methodology, Analytical Issues, and Interim Results, Argonne, Illinois, 2001, ESD/02-2.

6. Electric Power Research Institute, Advanced Batteries for Electric-Drive Vehicles, Palo Alto, California, 2003, 1009299.

7. National Academy of Sciences, Transitions to Alternative Transportation Technologies – Plug-In Hybrid Electric Vehicles, Washington, D.C., 2010, 12826.

8. United State Council for Automotive Research, <http://www.uscar.org>.

9. United States Advanced Battery Consortium, Electric Vehicle Battery Test Procedures Manual, Revision 2, Southfield, Michigan, 1996.

10. M. Coleman, W.G. Hurley, C.K. Lee, IEEE Trans. Energ. Convers. 23(2) (2008) 708-713.

11. M. Dubarry, V. Svoboda, R. Hwu, B.Y. Liaw, Electrochem. Solid-State Lett. 9(10) (2006) A454-A457.

12. N.A. Chaturvedi, R. Klein, J. Christensen, J. Ahmed, A. Kojic, IEEE Control Syst. 30(3) (2010) 49-68.

13. J. Vetter et al, Journal of Power Sources, 147 (2005) 269-281.

14. Electric Power Research Institute, Test Profile Development for the Evaluation of Battery Cycle Life for Plug-In Hybrid Electric Vehicles, Palo Alto, California, 2003, 1002228.

15. Electric Power Research Institute, Advanced Batteries for PHEVs: Sprinter PHEV Battery Testing, 2009 Update, Palo Alto, California, 2009, 1017675.

16. Partnership for a New Generation of Vehicles, PNGV Battery Test Manual, Revision 3, Idaho Falls, Idaho, 2001, DOE/ID-10597 Rev. 3.

17. National Renewable Energy Laboratory, Design of Electric Drive Vehicle Batteries for Long Life and Low Cost, Golden, CO, 2010, NREL/PR-540-48933.

18. D. Brown, M. Alexander, D. Brunner, S.G. Advani, A.K. Prasad, J. Power Sources 183 (2008) 275-281.

19. Idaho National Laboratory, Technology Life Verification Testing, Idaho Falls, ID, 2010, INEEL-EXT-04-01986.

20. Broussely, M., "Aging of Li-ion batteries and life prediction, an update," 3rd Int. Symposium on Large Lithium-Ion Battery Technology and Application, Long Beach, California, May 2007.

21. Hall, J., Lin, T., Brown, G., Biensan, P., and Bonhomme, F., "Decay processes and life predictions for lithium ion satellite cells," 4th Int. Energy Conversion Engineering Conf., San Diego, California, June 2006.

22. Smart, M., Chin, K., Whitcanack, L., and Ratnakumar, B., "Storage characteristics of Li-ion batteries," NASA Battery Workshop, Huntsville, Alabama, Nov. 2006.

23. Broussely, M., Chap. 13 in: *Advances in Lithium-Ion Batteries*, van Schalkwijk, W., and Scrosati, B., editors. New York: Kluwer Academic / Plenum Publishers, 2002.

24. GM Volt Specifications, http://gm-volt.com/full-specifications/, retrieved on 8-25-2011.

25. National Renewable Energy Laboratory Strategic Initiative Working Group Report: Thermal Model of Gen 2 Toyota Prius, Kandler Smith, Ahnvu Le, Larry Chaney.

26. National Renewable Energy Laboratory, Analysis of Off-Board Powered Thermal Preconditioning in Electric Drive Vehicles, Golden, CO, 2010, NREL/CP-5400-49252.

27. R.L. Polk & Co., https://polk.com.

28. National Renewable Energy Laboratory, National Solar Radiation Database, Typical Meteorological Year Database 3, Golden, CO.

29. 2001 National Household Travel Survey, http://nhts.ornl.gov/.

30. Society of Automotive Engineers, Recommended Practice for Measuring the Exhaust Emissions and Fuel Economy of Hybrid-Electric Vehicles, Including Plug-in Hybrid Vehicles, Hybrid Committee, 2010, J1711.

31. Society of Automotive Engineers, Utility Factor Definitions for Plug-In Hybrid Electric Vehicles Using 2001 U.S. DOT National Household Travel Survey Data, Hybrid Committee, 2009, J2841.

32. United States Environmental Protection Agency, Fuel Economy Labeling of Motor Vehicles: Revisions to Improve Calculation of Fuel Economy Estimates, Office of Transportation and Air Quality, 2006, EPA420-R-06-017.

33. Society of Automotive Engineers, Hybrid Electric Vehicle Fleet and Baseline Performance Testing, Presented at SAE 2006 World Congress & Exhibition, Detroit, Michigan, 10.4271/2006-01-1267.

34. United States Energy Information Administration, Annual Energy Outlook 2010: With Projections to 2035, Washington, DC., 2010, DOE/EIA-0383(2010).

35. F.R. Kalhammer, B.M. Kopf, D.H. Swan, V.P. Roan, M.P. Walsh, Status and Prospects for Zero Emissions Vehicle Technology: Report of the ARB Independent Expert Panel 2007, Prepared for State of California Air Resources Board, Sacramento, California, 2007, Final Report.

36. National Renewable Energy Laboratory, PHEV/EV Li-Ion Battery Second-Use Project, Golden, Colorado, 2010, NREL/PR-540-48018.

37. US Department of Energy, Office of Energy Efficiency and Renewable Energy, Vehicle Technologies Program, 2011 Annual Merit Review and Peer Evaluation Meeting, Energy Storage R&D, May 2011.